UNIVERSITEIT VAN PRETORIA
UNIVERSITY OF PRETORIA
YUNIBESITHI YA PRETORIA

BENEFICIATION OF ZIMBABWEAN PETALITE: EXTRACTION, PURIFICATION AND COMPOUND SYNTHESIS

By

Onias Sitando

A dissertation submitted in partial fulfilment
of the requirements for the degree

MSc: Applied Science (Chemical Technology)

Department of Chemical Engineering
Faculty of Engineering, Built Environment and Information Technology

Supervisor: Prof. Philip Crouse

University of Pretoria

February, 2012

DECLARATION

I, **Onias Sitando, student No. 29684995,** do hereby declare that this research is my original work and that to the best of my knowledge and belief, it has not been previously in its entirety or in part been submitted and is not currently being submitted either in whole or in part at any university for a degree or diploma, and that all references are acknowledged.

SIGNED on this _____ day of _____ 2012.

_____

Onias Sitando

SYNOPSIS

BENEFICIATION OF ZIMBABWEAN PETALITE: EXTRACTION, PURIFICATION AND COMPOUND SYNTHESIS

Author: **Onias Sitando**
Supervisor: **Prof. Philip Crouse**
Department: **Chemical Engineering**
Degree: **MSc: Applied Science (Chemical Technology)**

Lithium is one of the most strategically important minerals at the time of writing. The demand for lithium and lithium compounds to be used in lithium-ion batteries is increasing day by day. Zimbabwe possesses a considerable resource of lithium ore, estimated at 23 000 mt Li. Beneficiation of this lithium ore could indeed be a very promising business in the near future.

This work focuses on processing of petalite concentrate from the Bikita deposit in Zimbabwe for production of Li_2CO_3, with subsequent preparation of LiF and LiCl. Analysis performed on the petalite showed that the average Li_2O content is 4.10 %. The extraction method used involves roasting the pre-heated concentrate with concentrated H_2SO_4 followed by water leaching of the resulting Li_2SO_4, solution purification and precipitation of Li_2CO_3 with subsequent preparation of LiF and LiCl. Investigation of the roasting and leaching showed that the dissolution rates are significantly influenced by roasting temperature and stirring speed. 97.3 % optimum rate of extraction was attained at 320 rpm and roasting temperature of 300 °C. Water-washed lithium carbonate with a purity of 99.21 %(metal basis) and an average particle size of 1.4 µm was produced.

Good quality LiF and LiCl can be produced with purity of 99.36 % and 99.02 % respectively. The pH, concentration and agitation have a great influence on the morphology of the precipitated LiF. Lower pH values and optimum concentration of the Li_2CO_3 solution results in smaller particle size. High recovery of 96.53 % LiF was realised. Anhydrous LiCl was found to absorb moisture when exposed to air at

ambient temperature. The synthesised LiCl melts at 606.2 °C with a corresponding enthalpy of fusion of 18.4 kJ mol^{-1}, close to the values reported in the literature.

Keywords: Petalite; lithium; lithium extraction; leaching; lithium carbonate; Bikita Minerals; lithium fluoride and lithium chloride.

ACKNOWLEDGEMENTS

I would like to express my deepest appreciation to my supervisor, Professor Philip Crouse. His guidance, suggestions, advice and support throughout this work were of the utmost importance.

Further thanks go to Bikita Minerals (Pvt) Ltd for providing the petalite sample. Moreover, I would like to thank the University of Pretoria, the South African National Research Foundation (NRF) and the Flourochemical Expansion Initiative (FEI) for financial assistance.

I also owe a debt of gratitude to my friends at University of Pretoria for their selfless and untiring academic motivation. Notably those who deserve special mention are John, Ncamisile, Bola and Jain.

Finally, my heart-felt appreciations go to my loving wife, Monica and my blessed daughter and son, Mitchelle and Tatenda, for their understanding and perseverance.

Research outputs emanating from this dissertation

1. O. Sitando, P.L. Crouse (2011) “Processing of a Zimbabwean petalite to produce lithium carbonate”, *International Journal of Mineral Processing*, 102, 45-50.

2. O. Sitando, P.L. Crouse (2011) “Processing of a Zimbabwean petalite to produce LiF” paper presented at *11th International Conference on Polymers and Advanced Materials* (ICFPAM XI).

LIST OF FIGURES

Figure 1 Mineral deposits in Zimbabwe..... ……11

Figure 2 An outline of lithium chemicals produced from Li_2CO_3..... ……16

Figure 3 Lithium carbonate demand 2002-2022 18

Figure 4 Lithium consumption by end use 2002-2022 18

Figure 5 Metal hydroxide precipitates diagram 21

Figure 6 Flow sheet for Li_2CO_3 production from spodumene/petalite.....24

Figure 7 Flow sheet for leach liqour purification.....36

Figure 8 Flow sheet for precipitation of lithium carbonate.....37

Figure 9 Experimental setup of Li_2CO_3 carbonation 39

Figure 10 Particle size distribution of petalite concentrate 42

Figure 11 Effect of roasting temperature on the extraction rate of lithium 45

Figure 12 Effect of stiring speed on the extraction rate of lithium.....46

Figure 13 Effect of solid/liquid ratio on the extraction of lithium 47

Figure 14 Effect of leaching temperature on the extraction of lithium 48

Figure 15 Thermograms for synthesised and commmercial Li_2CO_3.....50

Figure 16 X-ray partterns for synthesised and commmercial Li_2CO_3 51

Figure 17 Particle size distribution of synthesised Li_2CO_3.....52

Figure 18 SEM images of LiF prepared at 25 °C.....53

Figure 19 SEM images of LiF at pH 5.0 ..... **54**

Figure 20 SEM images of LiF at pH 2.5 ..... **55**

Figure 21 SEM images of LiF at pH 1.0 ..... **55**

Figure 22 SEM images of LiF (25 g L^{-1} Li_2CO_3 solution) **56**

Figure 23 SEM images of LiF (50 g L^{-1} Li_2CO_3 solution) **57**

Figure 24 SEM images of LiF at 350 rpm **58**

Figure 25 SEM images of LiF at 0 rpm **58**

Figure 26 X-ray patterns for the snythesised and purchased Merck LiF **59**

Figure 27 (a) Commercial and (b) synthesised LiF powder **60**

Figure 28 Particle size distribution of synthesised LiF **61**

Figure 29 X-ray diffractogram of synthesised LiCl **62**

Figure 30 DSC-TG curves for synthesised LiCl **64**

Figure 31 DSC-TG curves for purchased Merck LiCl **65**

Figure 32 A schematic diagram of an X-ray diffractometer **79**

Figure 33 Scattered beam of X-rays **79**

Figure 34 X-ray fluorescence principle **81**

Figure 35 Schematic diagram of scanning electron microscope **83**

Figure 36 Schematic representation of an ICP-OES instrument **85**

Figure 37 Peristaltic pump **86**

Figure 38 Concentric neubulizer **87**

Figure 39 Spray chamber connnected to the neubilizer **88**

Figure 40 Schematic representation of the different zones in the ICP **89**

Figure 41 An image of a torch for Spectro Arcos **90**

Figure 42 A Schematic diagram for a thermobalance **92**

Figure 43 Integrated heat flow peaks for snythesied LiCl **95**

Figure 44 Integrated heat flow peaks for purchased LiCl **96**

LIST OF TABLES

Table 1 Some physical properties of lithium ..... ……6

Table 2 Composition of some lithium minerals ..... ……7

Table 3 Estimated international lithium reserves 10

Table 4 Estimate for the global lithium uses and percentages 17

Table 5 Solubility of lithium carbonate in water 27

Table 6 Some of the properties of LiF and LiCl 28

Table 7 Solubility of lithium chloride 29

Table 8 Semi-quantitative mineral content of the petalite 43

Table 9 Chemical composistion of the petalite 44

Table 10 Concentration of elements in processed solutions 49

Table 11 Concentration of impurities in lithium carbonate 52

Table 12 Contents of impurities in lithium fluoride 60

Table 13 Contents of impurities in lithium chloride 66

TABLE OF CONTENTS

Declaration statement ..... **i**

Synopsis ..... **ii**

Acknowledgements ..... **iv**

List of figures ..... **vi**

List of tables ..... **ix**

Chapter 1 Introduction 1

1.1 Background **1**

1.2 Motivation **2**

1.3 Objectives of the study **3**

1.4 Scope of the study **3**

Chapter 2 Literature review 5

2.1 Lithium and its properties **5**

2.2 Lithium sources **6**

2.2.1 Minerals **7**

2.2.2 Brines **9**

2.2.3 Clays **9**

2.3 Lithium reserves **9**

2.3.1 Bikita deposits in Zimbabwe **10**

2.4 Appplications of lithium and lithium compounds **12**

2.5 Lithium market 17

2.6 Lithium concentrate processing and impurity removal 19
2.6.1 Leaching fundamentals 19
2.6.2 Precipitaion fundamentals 20
2.6.3 Lithium extraction 22
2.6.2 Recovery of lithium from leach solution 26

2.7 Lithium chloride and lithium fluoride 28
2.7.1 Lithium chloride and lithium fluoride preparation 29

2.8 Toxicology of lithium and lithium compounds 32

2.9 Conclusions from the literature review 32

Chapter 3 Experimental work 33

3.1 Materials 33

3.2 Instrumentation 33

3.3 Methods 33
3.3.1 Particle size analysis 33
3.3.2 Characterisation of the concentrate 34
3.3.3 Calcination and roasting of petalite 34
3.3.4 Leaching stuidies 35
3.3.5 Solution purification 35
3.3.6 Precipitation of lithium from leach liquor 36
3.3.7 Characterisation of lithium carbonate 37

3.3.8 Preparation of lithium fluoride 38
3.3.9 Preparation of lithium chloride 40

Chapter 4 Results and discussion 42

4.1 Particle size distribution 42

4.2 Mineralogical composition of the concentrate 43

4.3 Elemental analysis of the concentrate 43

4.4 Roasting studies 45
4.4.1 Effect of roasting temperature and time 45

4.5 Leaching studies 45
4.5.1 Effect of stiring speed 45
4.5.2 Effect of solid/liquid ratio 46
4.5.3 Effect of leaching temperature and time 47

4.6 Solution purification 48

4.7 Precipitation and characterisation of lithium carbonate 49

4.8 Precipitation of lithium fluoride 53
4.8.1 Effect of temperature 53
4.8.2 Effect of pH 54
4.8.3 Effect of concentration 56
4.8.4 Effect of stirring 57

4.9 Characterisation of lithium fluoride 59

4.10 Characterisation of lithium chloride 61

Chapter 5 Conclusions and recommendations 67

5.1 Conclusions **67**

5.2 Recommendations **69**

References 70

Appendices 78

CHAPTER 1 INTRODUCTION

1.1 Background

Lithium is found in minerals, lake brines, clays, seawater and oil residues. One of the minerals of commercial importance is petalite ($LiAlSi_4O_{10}$) which is found, inter alia, in Bikita, Zimbabwe. Zimbabwe is among the leading lithium concentrate producing countries in the world and its lithium reserves are estimated at 23,000 mt Li (Jaskula, 2010). Other minor lithium deposits in Zimbabwe occur in the Insiza, Matobo, Mazoe, Mutoko, Harare, Mutare, Kamativi and Hwange districts (Cooper, 1964).

The mineral petalite is one of the commercial sources of lithium and lithium compounds, viz. lithium carbonate (Li_2CO_3), lithium fluoride (LiF) and lithium chloride (LiCl). Lithium carbonate is used in the glass and ceramic industry, in the aluminium industry and is used as a precursor for lithium cobalt oxide which is used in energy storage devices such as rechargeable lithium-ion batteries. High-purity lithium carbonate is used in the treatment of manic-depressive psychosis (Ober, 2007) and production of electronic grade crystals of lithium niobate (Amouzegar et al., 2000).

Lithium carbonate is the precursor for all other lithium compounds including lithium fluoride and chloride, a raw material for lithium metal production (Jandová, 2010). Lithium fluoride powder is used in the glass and ceramic industries, in the aluminum smelting process, as flux, and in UV optics. One of its most important modern applications is as a precursor for lithium hexafluoro-phosphate which is applied in the the battery industry. Lithium chloride, apart from lithium metal production is also used in industrial air-conditioning and commercial dehumidification of air.

Processing of lithium minerals relies on chemical roasting of the concentrate with the use of sulphuric acid (Kondás and Jandová, 2006; Wietelmann and Bauer, 2003), hydrochloric acid (Wietelmann and Bauer, 2003), limestone and or lime (Wietelmann and Bauer, 2003), sodium and or potassium salts and calcium sulphate with calcium hydroxide (Kondás and Jandová, 2006). The objective of all the processing techniques is to convert lithium minerals into soluble form. Roasting of lithium

minerals with H_2SO_4 gives a high yield of lithium and has favourable energy consumption compared with other processes (Wietelmann and Bauer, 2003). In addition, H_2SO_4 is cheaper and easier to handle than HCl. Roasting with HCl is not attractive because of complexity of purification. Wietelmann and Bauer (2003) reported that the alkaline process and other processes have a relatively high energy requirement and give a lithium yield appreciably below that of the sulphuric acid process.

Jaskula (2008) reported that the global market for lithium-ion batteries has increased by more than 20 % per year in the past few years and that the use of lithium-ion batteries in upcoming electric and hybrid vehicles could further increase demand for the metal. The growing demand for lithium to meet the raw material needs of the energy storage devices is one of the reasons for studying the upgrading of Zimbabwean petalite into Li_2CO_3, LiF and LiCl . In addition there is very limited work or published data, particularly on the chemical leaching and processing of Zimbabwean petalite. One major work is that of Cooper (1964), which was preliminary in nature and was on the geology of Bikita pegmatite and petalite characterisation. The work presented here is thus expected to be of interest.

This study gives detailed data on the characterisation, concentrate roasting with H_2SO_4, subsequent water leaching of the resulting Li_2SO_4, solution purification, and precipitation of Li_2CO_3 along with final synthesis of LiF and LiCl from the prepared lithium carbonate solution.

1.2 Motivation

Most of the petalite mineral mined at Bikita is used directly as ore concentrate in ceramics and glass applications in Zimbabwe and the surrounding region rather than feedstock for lithium carbonate and other lithium compounds. On the other hand, bulk prices have been reported to be as low as $147 per tonne of petalite concentrate (4.2 % Li_2O) compared to $6,600, $ 8,500 and $23,150 per tonne lithium carbonate, lithium chloride and lithium fluoride respectively (Ecceslestone, 2010).

This is one of the motivating factors for this study. Another additional motivating factor is that, Zimbabwe is among the largest producers of lithium concentrate in the world while its neighbour South Africa is third largest producer of fluorspar. These vital resources are and can be used for production of raw materials for synthesis of many chemical products including lithium cobalt oxide ($LiCoO_2$) and lithium hexafluorophosphate ($LiPF_6$), important components of lithium-ion batteries. Lithium carbonate consumption per 1 kWhr is estimated at 0.6 kg and the average battery capacity of an electric vehicle (Tesla) is 25 kWhr translating to a lithium carbonate equivalent of 15 kg (Chemetall, 2009).

1.3 The objective of the study

The objectives of the study are:

- To determine the influence of roasting conditions on the lithium conversion from petalite to a soluble compound;
- To investigate the effect of different leaching conditions on lithium extraction;
- To optimize the leaching conditions;
- To purify the leach solution;
- To study the Li_2CO_3 precipitation process from the purified leach solution with regards to yield and purity;
- To evaluate the synthesis of LiF and LiCl from prepared Li_2CO_3.

1.4 The scope of the study

The scope of this study encompasses the following:

- The use of petalite concentrate procured from Bikita Minerals (Pvt) Ltd;
- Particle size analysis of the petalite concentrate;
- Chemical analysis of the petalite using XRF and ICP-OES;
- Mineralogical studies of the concentrate using XRD;
- Determination of optimum roasting conditions;

- Experimental determination of optimum leaching conditions;
- Lithium solution purification;
- Recovery of lithium from purified leach solution as Li_2CO_3;
- Preparation of LiF and LiCl from Li_2CO_3;
- Characterization and comparison of commercial and synthesised Li_2CO_3, LiF and LiCl.

The Information search made use of the following databases and web search engines: Science direct, Scopus, Scifinder, Google and Yahoo. A Patent search was done using Espacent. The key words used were “lithium”, “lithium extraction”, “dissolution kinetics”, “leaching”, “Bikita minerals”, “lithium reserves”, “uses of lithium and its compounds”, “lithium carbonate”, “lithium chloride”, “lithium fluoride”.

2 LITERATURE REVIEW

In this review, papers presented mainly in the last three decades are considered. The review is systematised into six major sections. Section one deals with lithium and its properties and section two deals with world resources of lithium. The third section deals with applications of lithium and lithium compounds and the fourth section focus on processing of mineral concentrate and impurity removal techniques. The fifth section deals with precipitation of lithium as a carbonate and the last section focuses on preparation of lithium chloride and lithium fluoride. Lithium extraction is the major focus of this literature survey as it constitutes the main area of interest for this dissertation. A discussion of different methods for lithium extraction is given. The advantages as well as the limitations of these methods are reviewed.

2.1 Lithium and its properties

Lithium is a silvery white metal and is the lightest metal known to man. Lithium is an extremely reactive alkali metal particularly with oxygen. The name lithium comes from the Greek word “lithos”, meaning stone. Lithium was first detected and indentified by Johann August Arfvedson, one of Jöns Jakob Berzelius’s students, in 1817 while analyzing the mineral petalite (Kamiensiki et al., 2005). The metal was first extracted and recovered from lithium chloride through electrolysis in 1818 by Sir Humphrey Davy and William Thomas Brande (Wietelmann and Bauer, 2003). The first commercial production of lithium was by the Germany company Metalallgesellschaft AG in 1925 (Comer, 1978).

Lithium has made and will continue to make a vital contribution in sustaining and improving society due to its unique properties. Lithium is the most electronegative metal, the lightest metal with a molecular weight of 6.94 g mol^{-1} and the least dense metal with a density of 0.534 g cm^{-3}. Some of the physical properties of lithium are shown on Table 1 (Garrett, 2004; Bale and May, 1989).

Table 1. Some physical properties of lithium.

	Lithium
Atomic number	3
Atomic weight	6.94 g mol^{-1}
Crystal structure	b.c.c
Lattice constant	3.5 Å
Density	0.534 g cm^{-3}
Melting point	180.54 ℃
Boiling point	1347 ℃
Ionic radius	0.68 Å
Electron affinity	0.54 eV

In addition to the above physical properties, lithium has also some unique chemical properties. Lithium is very reactive. Molten lithium reacts explosively with water. Exposure of lithium ingots to air results in the reaction of lithium with atmospheric N_2 forming reddish brown colour of lithium nitride and can lead to ignition (Wietelmann and Bauer, 2003).

Lithium burns with a very luminous white flame, forming a dense smoke consisting mainly of lithium oxide with a flame temperature of almost 1100 °C (Wietelmann and Bauer, 2003). Burning lithium reacts with carbon dioxide and silicates (sand and concrete). These substances cannot be used as fire-fighting agents for lithium flames. Suitable fire-fighting agents for lithium are calcium carbonate and fire-extiquishing powders based on NaCl (Mcketta, 1988).

2.2 Lithium sources

Lithium is found in minerals, lake brines, clays, seawater and oil residues. It is the 27th most abundant element (Wietelmann and Bauer, 2003). The commercial sources of lithium are minerals and brines (Grady, 1980).

2.2.1 Minerals

About 150 lithium minerals are known (Wietelmann and Bauer, 2003), however only a few are of commercial importance. The main lithium minerals are shown in Table 2.

Table 2. Composition of some lithium minerals (Jandová et al., 2010; Garrett, 2004; Demirbas, 1999; Epstein et al., 1981).

Mineral	General formula	Li_2O %
Spodumene	$LiAlSi_2O_6$	6.0-7.5
Petalite	$LiAlSi_4O_{10}$	3.5-4.5
Lepidolite	$K[Li,Al]_3[Al,Si]_4O_{10}[F,OH]_2$	3.3-7.74
Zinnwaldite	$K[Li,Al,Fe]_3[Al,Si]_4O_{10}F_2$	2.0-5.0
Amblygonite	$Li,Al[F,OH]PO_4$	7.5-9.5
Eucryptite	$LiAlSiO_4$	4.5-6.5

- Petalite ($LiAlSi_4O_{10}$) is a monoclinic mineral with a framework silicate structure. Its colour is white, or greyish white, with a density of 2.4 g cm^{-3} and hardness of 6 Mohs. Petalite is generally associated with other pegmatites such as spodumene, eucrypite and lepidolite. It is one source from which lithium is produced commercially (Garrett, 2004). Natural petalite is resistant to chemical attack (Distin and Philips, 1982). Heating petalite at high temperatures converts it to tetragonal β-spodumene which is reactive to acid or base attack (Anovitz et al., 2006; Garrett, 2004; Bale and May, 1989; Grady, 1980). Large deposits of petalite occur in Bikita, Zimbabwe; Kenora, Ontario, Canada; Aracuai, Brazil; and Londonerry, Australia. A significant amount of petalite has also been reported in Karibib, Namibia (Roering and Gevers, 1964).

- Spodumene ($LiAlSi_2O_6$) is a monoclinic pyroxene with a density of 3.16 g cm^{-3}. It is the most important lithium ore mineral because its high lithium content, extensive deposits and easy processing (Garrett, 2004). Natural spodumene (α-spodumene) undergoes a irreversible phase change to a tetragonal β-spodumene on heating at about 1000-1100 ℃ which is more amen able to chemical attack (Averill and Olson, 1977). Spodumene deposits are found in: North America;

Greenbushes, Australia; Brazil; China; Krivoj Rog, Russia; and Manono, Zaire (Wietelmann and Bauer, 2003; Garrett, 2004).

- Lepidolite ($K[Li,Al]_3[Al,Si]_4O_{10}[F,OH]_2$) is a complex lithium mica with variable composition. It is mainly used directly as a concentrate for production of glasses and ceramics. It is pink to greyish violet and has a density of 2.8-3.0 g cm^{-3}. Lepidolite is mainly associated with potassium, rubidium and cesium and is an ore source of rubidium (Wietelmann and Bauer, 2003). The major commercial deposits of lepidolite are Bikita, Zimbabwe; Bernic Lake, Canada; Karibib, Namibia; Mina Gerais, Brazil; and Sociedad Mineria de Pegmatite, Portugal (Garrett, 2004).

- Amblygonite ($LiAl[F.OH]PO_4$) is a phosphate which when compared to silicates is relatively acid soluble (Distin and Philips, 1982). Amblygonite is milky white to grey in colour and has a density of 2.98-3.11 g cm^{-3}. Distin and Philips (1982) reported that sizeable deposits are rare. However, mining of amblygonite has been reported in Canada, Brazil, Surinam, Zimbabwe, Rwanda, Namibia, and the Black Hills in the United States (Garrett, 2004).

- Zinnwaldite ($K[Li,Al,Fe]_3[Al,Si]_4O_{10}[F,OH]_2$) is regarded as a variety of lepidolite with relatively high iron content (Kondás and Jandová, 2006). Significant reserves of zinnwaldite are located in Czech Republic and Massachusetts (Jandová and Kondás, 2006; Wietelmann and Bauer, 2003).

- Eucryptite ($LiAlSiO_4$) is a lithium mineral which occurs mainly in combination with petalite. It is less common and is found in Bikita, Zimbabwe (Wietelmann and Bauer, 2003).

2.2.2 Brine sources

Brines from lakes, salars, seawater, oil-field waters and geothermal waters are the largest sources of lithium and lithium chemicals (Wietelmann and Bauer, 2003). Lithium is present as LiCl in natural brines. Extraction of lithium is through natural leaching and concentration by evaporation of salty water using solar energy. This process requires less energy compared to extraction of lithium from minerals. Lithium brines are mainly processed in Chile, South America (Brandt and Haus, 2010). Brines are also found in Bolivia, Argentina, United States and Qinghai province in China (Kamiensiki et al., 2005).

2.2.3 Clays

An additional source of lithium is the lithium-bearing clays. One of these clays is hectorite ($Na_{0.33}[Mg,Li]_3Si4O_{10}[F,OH]_2$) which contains 0.7-1.3 % Li_2O and is found near Hector California (Averill and Olson, 1977). Major lithium clay deposits are found in Nevada, California, Utah, Oregon, Wyoming, Arizona and New Mexico (Garrett, 2004; Hamzaoui et al., 2003). Although lithium bearing clays are the third important source of lithium, there is no commercial production from clays because extraction is uneconomic compared to minerals and brines (Buyukburc et al., 2006; Averill and Olson, 1977).

2.3 Lithium reserves

The major producers of lithium concentrates in the world in 2009 are Australia, Canada, Zimbabwe, Portugal and Brazil (Jaskula, 2010). Pegmatite deposits in Zimbabwe contain significant amounts of lithium and Bikita pegmatite is one of the world's largest lithium deposits (Veasey, 1997). A pegmatite is an intrusive igneous rock composed of interlocking mineral grains. Table 3 summarises the world's major reserves of lithium (Jaskula, 2010).

Table 3. Estimated international lithium reserves.

Country	Reserves (1000 mt Li)
Chile	7500
Argentina	800
Australia	580
China	540
Brazil	190
Canada	180
United States	38
Zimbabwe	23

2.3.1 Bikita deposits in Zimbabwe

This study focuses on the processing petalite concentrate from Bikita area in Masvingo province, Zimbabwe. The Bikita pegmatite area is located 64 km north east of Masvingo. The location of the Bikita lithium mine is denoted by “Li” in Figure 1(Mobbs, 1995).

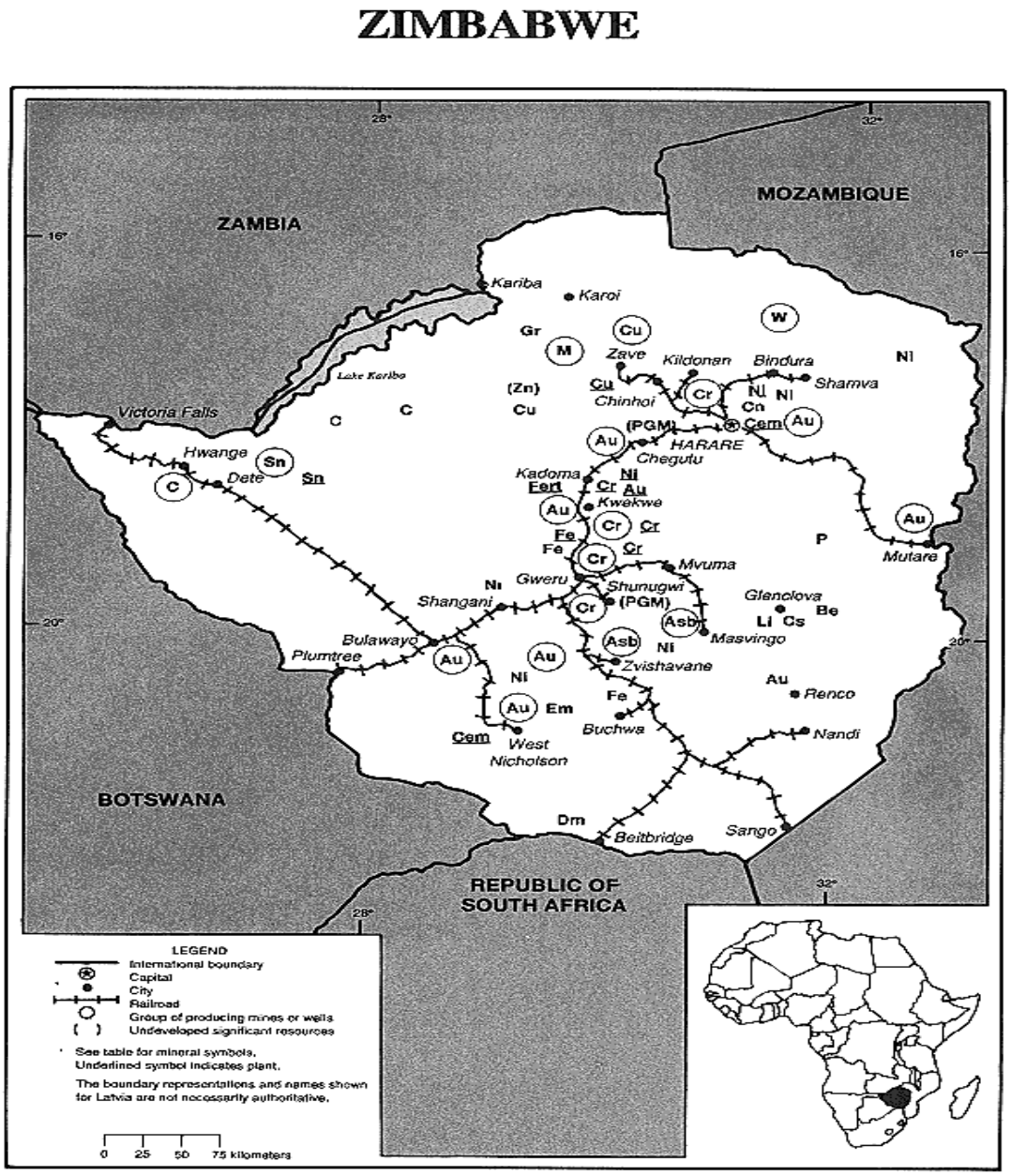

Figure 1. Mineral deposits in Zimbabwe.

The Bikita pegmatite area is divided into the Al Hayat, Bikita, Southern and Nigel sectors, and it is distinctly zoned. The largest deposits of petalite occur in the Al Hayat sector where very large crystals of low-iron (0.03 % Fe_2O_3) petalite occur with massive microline (potassium feldspar) in a matrix of fine-grained albite (Garrett, 2004). The petalite occurs as laths up 1.8 m long and 46 cm wide. The Bikita sector

was original dominated with lepidolite (most of it has been mined). It also has large amounts of spodumene, petalite, and amblygonite (Cooper, 1964).

The Bikita pegmatite area has an unusual variety and tonnage of commercial lithium minerals, as well as tantalum, tin, beryl and pollucite (Garrett, 2004). Its reserves was estimated to be 6 million ton Li in 1961 (Cooper, 1964) and 23, 000 mt Li in 2009 (Jaskula, 2010).

Other minor lithium deposits in Zimbabwe occur in the Insiza, Matobo, Mazoe, Mutoko, Harare, Mutare, Kamativi and Hwange districts (Cooper, 1964).

2.4 Applications of lithium and lithium compounds

Lithium chemicals are essential in many branches of industry. Its oldest application is in the glass and ceramic industry. The addition of lithium carbonate or lithium concentrate in glass and ceramic production lowers the process melting point, reduces energy consumption, increases furnace refractory life, improves the strength of the glass product, and reduces the coefficient of thermal expansion as well as viscosity (Ebensperger et al., 2005; Garrett, 2004). Petalite from Bikita Mineral (Pvt) Ltd, because of its low iron content, has been one of the dominant sources of lithium concentrate for direct use in the glass and ceramic industry (Garrett, 2004). The petalite crystal does not accommodate very much iron (Fe), so its deposits have very low iron content. Earlier publication by Cooper (1964) on petalite from Bikita Minerals (Pvt) Ltd showed an Fe_2O_3 content of 0.05 %.

Lithium has recently found use in energy storage devices such as rechargeable lithium ion batteries and extra demand for lithium is anticipated in the near future (Brandt and Haus, 2010). Lithium is the most electronegative of all the metals, with a standard electrode potential of 3.045 V, meaning it can generate the greatest power per unit mass compared to other metals (Garrett, 2004). Lithium ion batteries are lighter, have longer shelf life and they do not have a “memory effect” problem (i.e.

the amount of energy stored decreasing if the battery is charged before being fully discharged). Owing to these merits lithium ion batteries are now the preferred energy storage devices for laptops, camcorders, mobile phones and other portable electrical devices.

Jaskula (2008) reported that the global market for lithium ion batteries has been increasing by more than 20 % per year in the past few years and that the use of lithium batteries in upcoming electric and hybrid vehicles could further increase demand for the metal. Non-rechargeable lithium ion batteries are also used in calculators, cameras, watches and other devices.

Apart from its standard use in the glass and ceramic industry, lithium compounds are used as catalysts and reagents in the production of synthetic rubbers, plastics and pharmaceuticals. N-butyllithium is used to initiate the reaction between styrene and butadiene to form abrasion-resistant synthetic rubbers (Garrett, 2004). Lithium metal is also used as a catalyst in the production of pharmaceutical drugs such contraceptives, steroids, tranquilizers, vitamin A and anticholesterol agents, while lithium carbonate is used in the treatment of manic-depressive psychosis (Ober, 2007).

Lithium is also used to make aluminium-lithium alloys for wings and other parts of aircraft to reduce weight, allowing significant fuel saving during the lifespan of the aircraft. Ober (2007) reported that lithium has also found use as a concrete additive to prevent or mitigate premature deterioration of concrete through alkali silica reactivity.

Other lithium compounds, lithium bromide and lithium chloride, have found use in industrial air-conditioning and commercial dehumidification of air because of the low vapour pressure of their solutions, low viscosity and high stability. Both lithium bromide and chloride are extremely hygroscopic and can remove moisture from air producing a cooling effect (Garrett, 2004). The use of lithium chloride as humidistat

for drying of gases has also been reported (Conde, 2004). Lithium chloride is used as a component of fluxes and dipping bath for welding and brazing aluminium and light metals alloys (Ebensperger, 2005; Wietelmann and Bauer, 2003). Lithium hypochlorite is used as sanitizer for swimming pools (Epstein et al., 1980). In swimming pools it provides excellent sanitation while minimising algae growth. Lithium chloride also serves as an electrolyte in the reprocessing of spent nuclear fuel (Karell et al., 2001)

Lithium fluoride is used as flux for glasses, enamel and glazes and imparts a lower coefficient of expansion to glasses. Nano-powder lithium fluoride is applied in dosimetery for recording ionising radiation exposure from gamma rays, beta particles and neutrons (Sarraf-mamoory et al., 2007). One of the most important applications of lithium fluoride is in the battery industry where it is used as a precursor for preparation of lithium hexafluorophosphate, an electrolyte used in lithium ion batteries. Lithium fluoride crystals are also applied in UV optics because they possesses the highest UV transmission of all the material.

Lithium hydroxide monohydrate is applied in the grease industry. Lithium based greases have good lubricating properties over a wide range of shear and temperatures, ranging from -15 to 200 °C (Garrett, 2004). In addition they have good resistance to water, hardening and oxidation. These greases have found use in aircrafts, the automotive industries, as well as marine and military equipment (Ober, 2007). Lithium hydroxide is employed in dyes and pigments as an additive for increasing solubility in dyestuffs and increasing brilliance of pigments. Lithium hydroxide is also used as a precursor for preparation of lithium chloride and lithium fluoride (Kamiensiki et al., 2005).

In the aluminium industry, lithium carbonate is added during electrolysis of alumina (Al_2O_3) to lower the melting point of the cryolite bath allowing a lower operating temperature for the cells, increasing the electrical conductivity, decreasing the bath viscosity, reducing the consumption of cryolite, reducing the consumption of anode

carbon and reducing fluorine emissions from the electrolytic cells (Ober, 2007; Ebensperger et al., 2005; Grady, 1980; Nicholson, 1978). Lithium carbonate reacts with the cryolite (Na_3AlF_6) in the cell to form lithium fluoride which has a very high fluxing ability, high electrical conductivity and low volatility (Garrett, 2004).

Lithium metal has also found use in the metallurgical industry, where it is used to remove gases (degas) from aluminium, copper and bronze. This process purifies the metal and improves its electrical conductivity (Garrett, 2004). Lithium chloride is used in flux welding powders and welding rod coating for metals difficult to weld such as steel and aluminium where they reduce the flux melting temperature and surface tension and increase the metal wetability. Lithium hydroxide can reduce the premature deterioration of concrete because of its stronger reactivity with silica (Garrett, 2004).

Lithium carbonate is the starting material for the industrial production of all other lithium compounds, including lithium chloride, the raw material for lithium metal production (Jandová, 2010, Wietelmann and Bauer, 2003). Figure 2 summarises lithium chemicals produced from lithium carbonate.

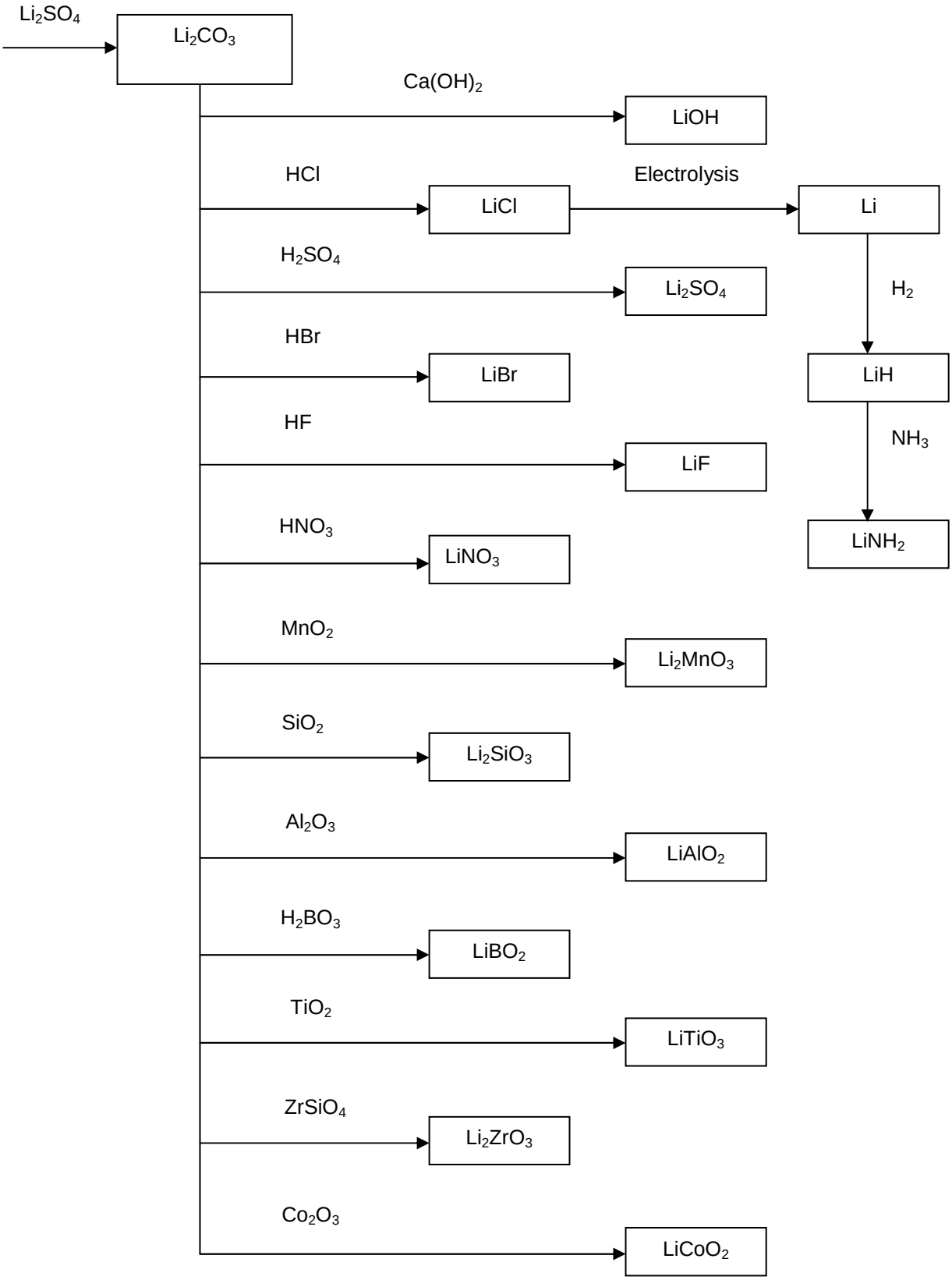

Figure 2. An outline of lithium chemicals produced from lithium carbonate.

One recent estimate of the percentages of global lithium uses for 2009 is shown in Table 4 (Jaskula, 2010).

Table 4. Estimate for the global lithium uses in percentages.

Application	%
Ceramics and glass	31
Batteries	23
Lubricating greases	10
Air treatment	5
Continuous casting	4
Primary aluminium production	3
Other uses	24

2.5 Lithium market

The demand for lithium and lithium compounds driven by secondary (rechargeable) batteries and Electric Vehicles (EV) batteries is increasing. Anderson (2009) reported that the demand for lithium, measured as Lithium Carbonate Equivalent (LCE) was around 110, 000 tpa in 2009 and is expected to rise to around 250, 000 to 300, 000 tpa in 2020 as shown in Figure 3.

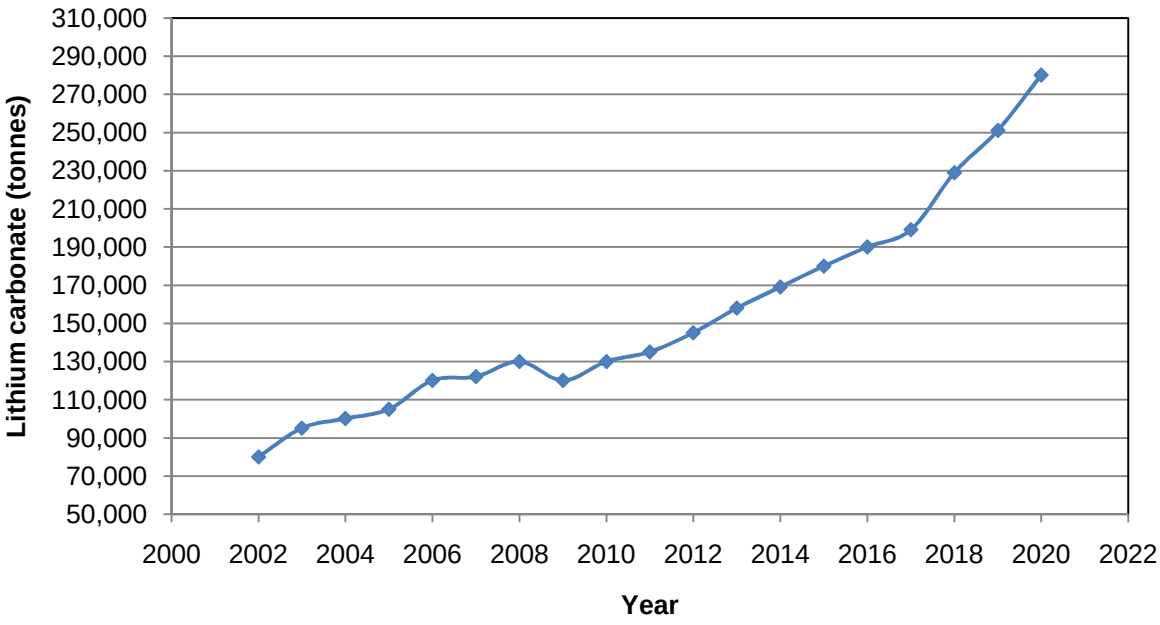

Figure 3. Total lithium carbonate demand 2002-2020.

Anderson (2009) also reported that the main drivers for the growth in the lithium consumption in the next ten years will be the battery sector and Li alloy production particularly in light aluminium alloys for the aerospace industry. Figure 4 shows the consumption of lithium by end use.

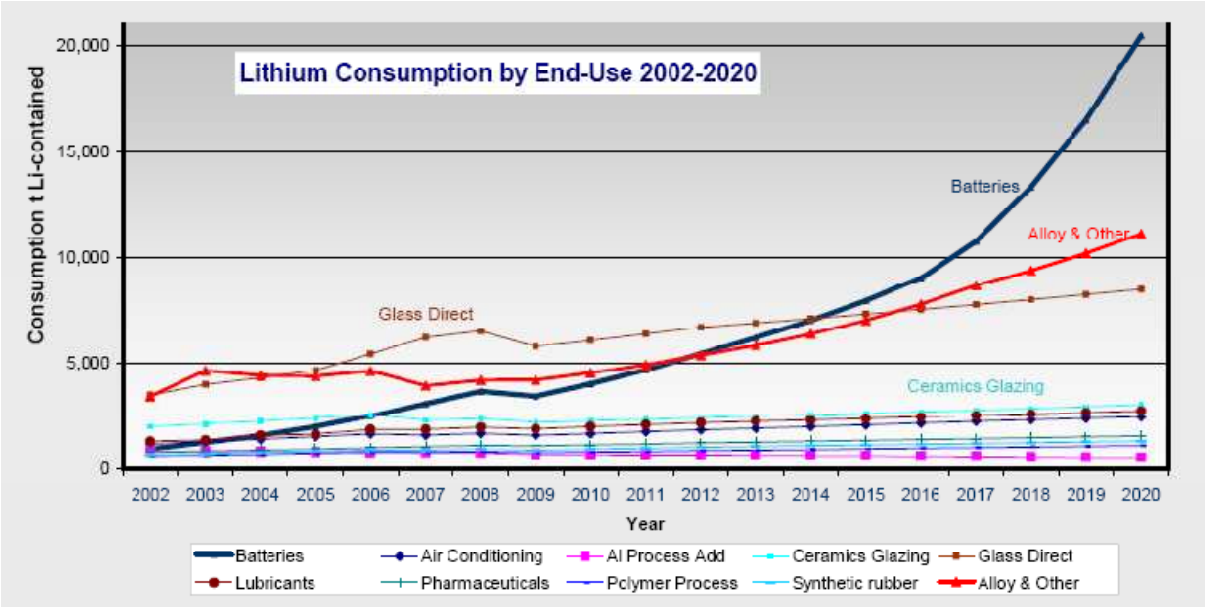

Figure 4. Lithium consumption by end use 2002-2020 (Adapted from Anderson, 2009).

2.6 Lithium concentrate processing and impurity removal

Lithium is an alkali metal, very reactive and very strong reducing agent. The usual methods of mineral extraction cannot be used in the extraction of lithium because of the following reasons (Habashi, 1997; Thorpe, 1922):

- It cannot be isolated by reduction of its oxides or other compounds, as it is very strong reducing agent.
- Alkali metals cannot be extracted from the ores by the electrolysis of their aqueous solutions, as the formed metal will immediately react with water giving their hydroxides instead.
- Lithium and all other alkali metals react violently with water, they burn or even explode. These metals cannot be prepared from any aqueous solution of its salt by the normal displacement methods.

Lithium metal is generally isolated by the electrolysis of fused metal halides. Lithium is extracted from mineral ore as lithium carbonate followed by synthesis of lithium chloride.

2.6.1 Leaching fundamentals

Leaching is the dissolution of a soluble component of an ore, concentrate, calcined product, or another intermediate by means of a solvent (Jackson, 1986). The rate of leaching of lithium is affected by a number of factors which includes particle size, the nature of the solvent, temperature and agitation.

- The solvent used should be selective and its viscosity should be sufficiently low for it to circulate freely. HCl is a very aggressive leaching agent that also dissolves a lot of impurities in the process. H_2SO_4 and water are less aggressive and hence more selective that HCl.
- Particle size influences extraction since smaller particles sizes result in greater interfacial area between the relevant solid and liquid. The diffusion of the solute through the porous structure of the residential solids is also shorter. Amer (2008) studied the effect of particle size on lithium conversion and found

that particle size can improve lithium dissolution rate. Small particles may, however, impede circulation of the liquid and separation of the particles from the liquid making subsequent drainage of the solid residue more difficult (Coulson and Richardson, 1996). In addition, the grinding costs also increase with the decrease in particle size.

- Temperature has a significant effect on lithium dissolution rate. In most cases higher temperatures results in a higher extraction rate of the metal in the solvent (Coulson and Richardson, 1996). Higher temperatures lower viscosity and increase diffusivity and thereby increase the rate of extraction.
- Agitation of the fluid is important because it prevents sedimentation and allows more active use of the interfacial surface (Coulson and Richardson, 1996). Stirring of the solvent increases the eddy diffusion hence the transfer of material from the surface of the particles to the bulk of the solution (Levenspiel, 1972).

2.6.2 Precipitation fundamentals

Acid roasting and leaching of calcinated lithium concentrate is not entirely selective as co-dissolution of impurities also occurs. Impurity removal is therefore necessary. Metal ions are usually removed or precipitated from solution as hydroxides, carbonate or sulphides (Jackson, 1986). Precipitation is the formation from solution of a solid product as a result of dilution or addition of a reagent to the solution (Jackson, 1986). A precipitation process can be used to separate metal or a group of metals either for the purpose of removing impurities or for the recovery from solution of the major metal.

The thermodynamics of any metal salt dissolution reaction is governed by solubility product, K_{sp}.

$$Me(OH)_n \rightleftharpoons Me^{n+} + nOH^- \quad (1)$$

$$K_{sp} = [Me^{n+}][OH^-]^n \quad (2)$$

The square brackets indicate activity, Me is the metal and n is the stoichiometric coefficient. Precipitation of a salt is favoured once the solubility product (K_{sp}) of the concentration of the constituting ion is exceeded.

The region of solubility of metal hydroxides is conveniently plotted on a log [Me^{n+}] vs pH plot as shown on Figure 5 (Jackson, 1986). Each metal is soluble to the left of its line and insoluble to its right.

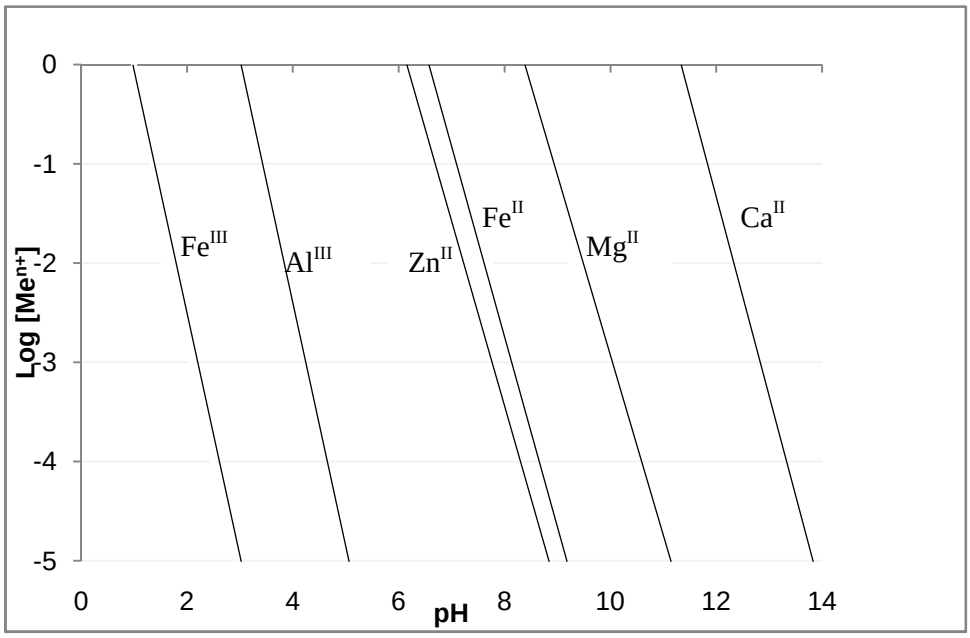

Figure 5. Metal hydroxides precipitation diagram.

The solubility product (K_{sp}) has to be exceeded to certain degree before noticeable precipitation can be observed. This phenomenon is referred to as supersaturation and it is defined by equation (3) (Jackson, 1986).

$$\sigma = \frac{C - C^*}{C^*} \tag{3}$$

σ is the relative supersaturation, C is the concentration of the substance to precipitate and C^* is the equilibrium solubility. The particle size of a precipitate is

largely determined by the relative supersaturation at the moment of precipitation (Jackson, 1986). If the solubility of a salt is suddenly exceeded through the addition of a chemical, high supersaturation will result in a rapid nucleation and formation of fine, poorly filterable precipitate. It is therefore important to have a controlled addition of a precipitation reagent. For the formation of a crystalline precipitate of coarse particle size, the relative supersaturation should be kept as small as possible at the time of nucleation. This can be achieved by inducing precipitation from hot, dilute solutions (Jackson, 1986).

An important practical aspect of precipitates is the subsequent necessity to separate the precipitate from the solution. This is achieved by filtration and the precipitate is usually freed from the remaining solution by washing with water or some suitable dilute electrolyte solution.

Hydroxide precipitation is a well established and simple technology that is relatively inexpensive compared to other processes such as solvent extraction.

2.6.3 Lithium extraction

A number of processes for the extraction of lithium from minerals exist in the literature. The basis of all the processes is to convert lithium minerals into soluble form. Although other mineral such as amblygonite and lepidolite can be treated directly with a digestion or roasting agent, petalite and spodumene require pre-treatment at high temperatures to convert α-spodumene and petalite to β-spodumene. β-spodumene is reactive to acid or base attack (Garrett, 2004; Bale and May, 1989; Grady, 1980).

Basic methods for processing of lithium minerals are as follows:

- Acid digestion (sulphuric acid process) is based on the decomposition of the material with H_2SO_4 at 250-400°C (Kondás and Jandová, 2006; Wietelmann and Bauer, 2003). The reaction of β-spodumene with H_2SO_4 is shown by equation (4) (Mcketta, 1998).

$Li_2O.Al_2O_3.4SiO_2(s) + H_2SO_4(conc) \rightarrow Li_2SO_4(s) + Al_2O_3.4SiO_2(s) + H_2O(g)$ (4)

The product is neutralised with limestone, leached with water and then separated by filtration. The resulting leach liquor contains aluminium, calcium, magnesium, iron and other impurities which can be removed by pH control and addition of a carbonate (Garrett, 2004; Averill and Olson, 1977). Lithium is extracted as lithium carbonate from the purified solution.

Wietelmann and Bauer (2003) reported that digestion of lithium minerals with H_2SO_4 gives a high yield of lithium and has relatively favourable energy balance compared with other processes. Jandovà et al. (2010) reported high lithium extraction of 70 to 97 % depending on the processed lithium mineral. The use of HCl for roasting is undesirable as HCl is a highly aggressive leaching agent which dissolves most of the impurities making purification much more complex. Corrosion problems are also severe.

Digestion of lepidolite by HCl or hydrogen gas at 935 °C has been suggested for the production of lithium chloride (Mcketta, 1988). However this process requires high temperatures and has little significance compared to the sulphuric acid process.

Sulphuric acid digestion is the commercial method of choice for processing petalite and spodumene (Garrett, 2004). Kondás and Jandová (2006) reported that this method is also suitable for processing of lepidolite, amblygonite or zinnwaldite. A typical flow sheet for the production of lithium carbonate from petalite or spodumene using sulphuric acid is shown on Figure 6 (Wietelmann and Bauer, 2003).

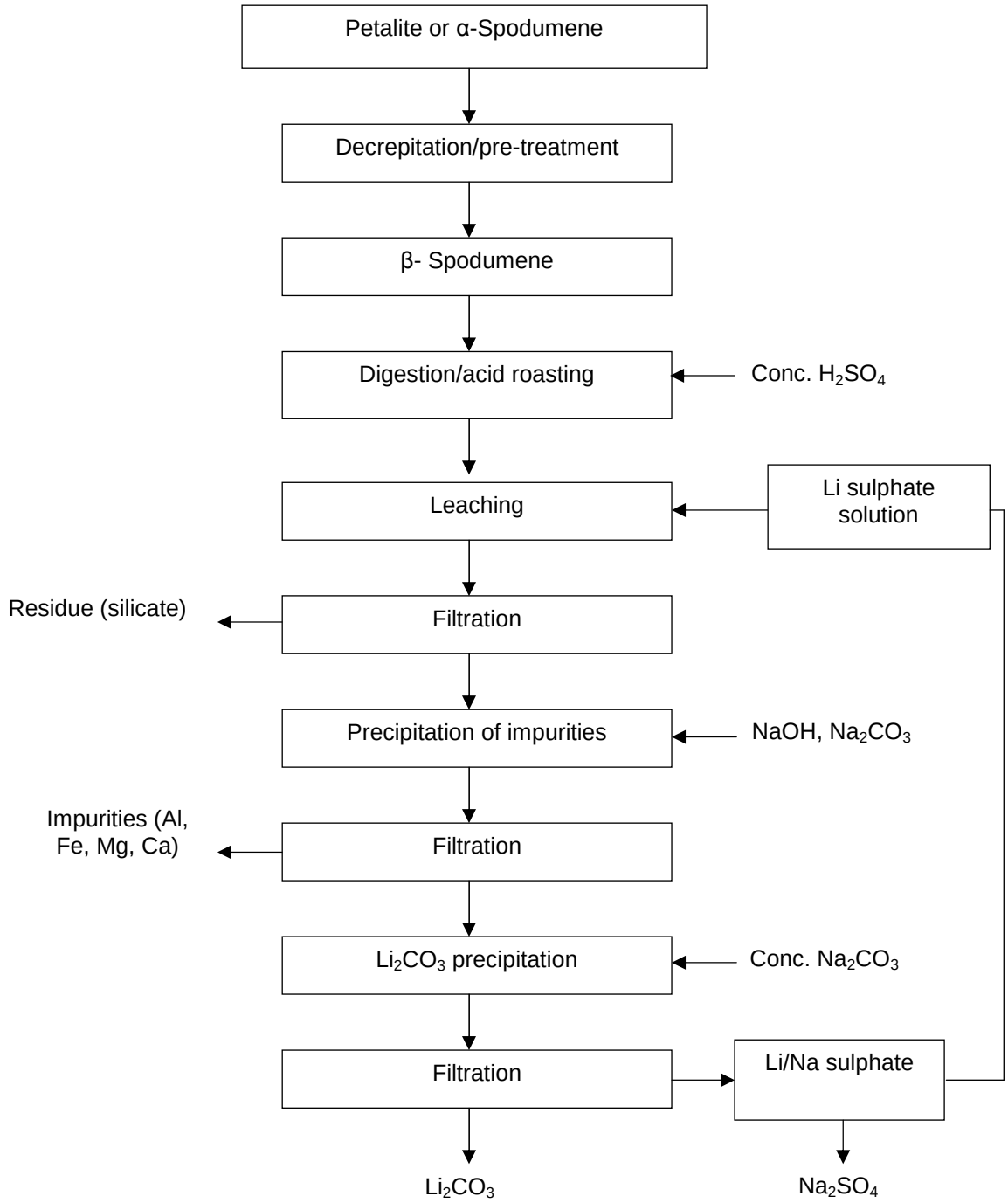

Figure 6. Flow sheet for lithium carbonate production from spodumene/petalite.

- Alkaline digestion (Limestone, Lime Roast Leach Process) is suitable for thermal decomposition of spodumene, petalite or lepidolite by treatment with limestone and or lime. Pre-heating, calcination and digestion are done as a single operation. The resulting clinker is ground and leached with water. The process is highly temperature dependent and for spodumene or petalite the process is carried out at 1040 °C (Wietelmann and Bauer, 2003). Too high temperature results in the formation of a glassy clinker which severely hinders subsequent leaching of lithium hydroxide and too low a temperature leads to incomplete reaction. The alkaline process has a relatively high energy requirement and gives a lithium yield appreciably below that of the sulphuric acid process (Wietelmann and Bauer, 2003).

- The sulphate process is a method used for processing of lepidolite and clays. Its basis is high temperature decomposition of lithium mineral by potassium and or sodium sulphate (Kondás and Jandová, 2006). The product is water-soluble lithium sulphate.

- Ion exchange process is another process which is based on either heating a lithium ore with a sodium and or potassium salt (Wietelmann and Bauer, 2003) or advanced hydrothermal decomposition in solution containing Na_2CO_3, NaOH or Na_2SO_4 at elevated temperatures and high pressures (Kondás and Jandová, 2006). The heating process leads to the replacement of Li^+ by Na^+ or K^+ from the silicate matrix. A water-soluble lithium salt of the anion used is formed. Long reaction time and high pressures makes the process unattractive compared to the acid digestion process. Anovitz et al. (2006) reported a reaction time of 3 days for the reaction of spodumene with 50 % NaOH at 200 °C in a pressure vessel.

- The gypsum process is used mainly for the decomposition of lepidolite and zinnwaldite by treatment with a mixture of calcium sulphate with calcium oxide and or calcium hydroxide (Jandová et al., 2008). The product is water-soluble lithium sulphate.

2.5.4 Recovery of lithium from leach solution

Recovery of lithium from pregnant solution after leaching of lithium has been studied (Jandová et al., 2010; Wang et al., 2009; Amer, 2008; Garrett, 2004) and even practised industrially (Garrett, 2004). Precipitation of lithium as lithium carbonate (Li_2CO_3) is used to recover lithium from the leach liquor.

Lagos and Becerra (2005) reported that precipitation with sodium carbonate is the most effective since sodium sulphate that also precipitates is eliminated by washing with hot water. Carbon dioxide was found to be less effective due to very slow reaction kinetics. Ammonium carbonate results in the coprecipitation of ammonium sulphate ($(NH_4)_2SO_4$) which is not eliminated by washing with water. Alvani et al. (2002) tested the three precipitating agents and reported that best results were achieved using Na_2CO_3.

Lithium carbonate is precipitated from lithium sulphate or lithium chloride solution according to the following equations:

$$Li_2SO_4(aq) + Na_2CO_3(aq) \rightarrow Li_2CO_3(s) + Na_2SO_4(aq) \quad (5)$$

$$2LiCl(s) + Na_2CO_3(aq) \rightarrow Li_2CO_3(s) + 2NaCl(aq) \quad (6)$$

Precipitation of sodium carbonate from lithium sulphate is the preferred route. Burkert et al. (1970) reported that it is much more difficult to obtain Li_2CO_3 with good settling, filtering and washing characteristics when working with LiCl solutions than when working with lithium sulphate. This is because the NaCl increases the solubility of Li_2CO_3. According Burkert et al. (1970) a small increase in NaCl concentration increases the solubility of Li_2CO_3 from 7.5 g L^{-1} to about 9.3 g L^{-1}.

In the precipitation of Li_2CO_3 from Li_2SO_4 solutions a dense precipitate, with good settling, filterability and washing properties is obtained. However the following conditions and considerations are important.

- The solubility of Li_2CO_3 in water or salt solutions decreases with an increase in temperature. To minimize solubility losses precipitation is carried out at 95-100°C (Zhang et al., 1998). Table 5 shows the variation of lithium carbonate with temperature (Wietelmann and Bauer, 2003).

Table 5. Solubility of lithium carbonate in water.

Li_2CO_3 (g) per 100 g water	
T (℃)	Solubility
20	1.33
25	1.29
30	1.25
40	1.17
50	1.08
60	1.01
80	0.85
100	0.72

- The use of approximately 15 % excess Na_2CO_3 over the stoichometric amount is desirable. An increase in carbonate ion concentration lowers the solubility of Li_2CO_3.
- Concentration of reactants is very important since Li_2CO_3 has an appreciable solubility in the mother liquor of the reaction; hence it is desirable to operate with rather concentrated solutions. Jandová et al. (2009) reported that at least 9 g L^{-1} Li is necessary to achieve acceptable precipitation efficiency.
- The reaction between lithium sulphate and sodium carbonate is only possible at high pH values. pH between 8 and 9 is ideal for lithium carbonate precipitation (Garrett, 2004; Lagos and Becerra, 2005).
- The precipitate formed has to be washed at least three times with hot water to eliminate Na_2SO_4 and excess Na_2CO_3.

From the literature survey it is clear that the sulphuric acid process is the mostly widely used because of the merits associated with it. Although the alkaline method seems short compared to the sulphuric acid process, the method is highly temperature dependent which makes it commercially non-viable. Based on these findings, the sulphuric acid process was chosen for the processing of the Zimbabwean petalite in this study.

2.7 Lithium chloride and lithium fluoride

Lithium chloride and lithium fluoride are some of the most important lithium compounds that are produced directly from lithium carbonate as shown in figure 2 above. Most of the applications of lithium chloride and lithium fluoride has been discussed in 3.2.3.

Lithium chloride and lithium fluoride, like most lithium based salts, are characterised by relatively low melting points and high ionic conductivity (Kamali et al., 2011). Table 6 below shows some the properties of the two lithium salts (David, 2009; Kamiensiki et al., 2005).

Table 6. Some of the properties of LiCl and LiF.

Property	**LiCl**	**LiF**
Melting point	610 ℃	845 ℃
Boiling point	1382 ℃	1681 ℃
Solubility in water	83.2 g/100 mL (25 ℃)	0.133 g/100 g (25.4 ℃)
Crystalline form	Cubic	Cubic
Density	2.068 g cm^{-3}	2.635 g cm^{-3}
Appearance	White solid	White powder
Enthalpy of fusion	19.8 kJ mol^{-1}	27.09 kJ mol^{-1}
Specific heat capacity	67.8 J mol^{-1} K^{-1}	38.1 J mol^{-1} K^{-1}

Apart from the above properties, LiCl is highly soluble in alcohol and hygroscopic (Garrett, 2004) while LiF is insoluble in alcohol and non hygroscopic.

Lithium chloride is very sensitive to moisture and will easily absorb water in humid atmospheres (Kamali et al., 2011). At temperatures below 100 ℃ the hydrates $LiCl.H_2O$ and $LiCl.2H_2O$ precipitate out as shown on table 7 (Kamiensiki et al., 2005).

Table 7. Solubility of lithium chloride.

Temperature ℃	Lithium salt, wt %	Solid-phase formula
0.0	40.2	$LiCl.2H_2O$
19.4	45.2	$LiCl.2H_2O$ + $LiCl.H_2O$
20.0	45.2	$LiCl.H_2O$
50.0	48.3	$LiCl.H_2O$
80.0	53.0	$LiCl.H_2O$
90.0	56.0	$LiCl.H_2O$ + LiCl
100.0	56.3	LiCl

The hydration of LiCl at temperatures ranging from -20 to 20 ℃ can be shown in equation (7) (Kamali et al., 2011).

$$LiCl_{solid} \xrightarrow{H_2O} LiCl_{solid} + LiCl.H_2O_{Solid} + \xrightarrow{30\ wt\%\ H_2O} LiCl.H_2O_{Solid} + LiCl.2H_2O_{Solid} \xrightarrow{47\ wt\%\ H_2O} LiCl.2H_2O_{Solid} + Liquid \xrightarrow{60\ wt\%\ H_2O} Liquid \quad (7)$$

2.7.1 Lithium chloride and lithium fluoride preparation

Lithium chloride can be prepared directly by digestion of some lithium minerals with HCl (Mcketta, 1988). Production of lithium chloride from minerals by HCl digestion is not the preferred route as this process has high energy consumption and complexity of purification. Direct production of lithium chloride from ore has not however been practised commercially (Wietelmann and Bauer, 2003). The other alternative method has been described for production of LiCl by direct chlorination of Li_2CO_3 by Cl_2 at 300-650 °C (Amouzegar et al., 2000). The method, however, requires a high temperature. The most common and preferred route for preparation of lithium chloride is the reaction of lithium carbonate or lithium hydroxide with HCl and the LiCl

recovered either as concentrated solution or dry product by evaporation (Kamiensiki et al., 2005; Garrett, 2004). The lithium carbonate can be either in the form of filter cake or powder.

Lithium chloride is highly corrosive. A rubber lined reactor and stirrer are ideal to use in lithium chloride production (Garrett, 2004). Specialised steel or nickel equipments can also be used (Wietelmann and Bauer, 2003). Lithium chloride both as a concentrated solution or anhydrous product is very hygroscopic and has to be packed in air tight containers. The anhydrous form serves as a feed material in the electrolytic production of lithium metal (Garrett, 2004).

Lithium fluoride is prepared from the reaction of hydrofluoric acid (HF) with lithium hydroxide (Sarraf-Mamoory et al., 2007, Kamiensiki et al., 2005) or lithium carbonate (Kamiensiki et al., 2005; Friedrich et al., 1999). Lithium carbonate is either reacted with HF to form LiF(aq) with solid powder recovered by evaporation or is first dissolved with carbon dioxide followed by precipitation of LiF with HF (Friedrich et al., 1999). The latter has the advantage of less energy consumption as it is carried out at room temperature and particle size can be controlled easily by varying the precipitation parameters. In addition, after the carbonation of Li_2CO_3 some of the insoluble impurities such as iron, magnesium and calcium are removed by physical means such as filtration and centrifugation (Amouzegar et al., 2000). Moreover, direct carbonation of Li_2CO_3 by pure CO_2 will not introduce other impurities (Yi et al., 2007). Based on these findings the method for preparing LiF by first dissolving lithium carbonate with carbon dioxide was chosen.

The mechanism and kinetics of the carbonation of Li_2CO_3 has been studied (Yi et al., 2007). The reaction mechanism involved in the process according to Yi et al. (2007) is as follows:

$$CO_2(s) + H_2O(l) \rightleftharpoons H_2CO_3(aq) \rightleftharpoons HCO_3^-(aq) + H^+(aq) \quad (8)$$

$$Li_2CO_3(s) + H^+(aq) \rightarrow 2Li^+(aq) + HCO_3^-(aq) \quad (9)$$

$$Li^+(aq) + HCO_3^-(aq) \rightleftharpoons Li^+(aq) + HCO_3^-(aq) \rightleftharpoons LiHCO_3(aq) \quad (10)$$

The overall reaction is as follows:

$$Li_2CO_3(s) + H_2CO_3(aq) \rightarrow 2LiHCO_3(aq) \quad (11)$$

The insoluble carbonate thus goes into solution as a bicarbonate.

2.8 Toxicology of lithium and lithium compounds

Lithium is more toxic than sodium. Wietelmann and Bauer (2003) reported that 5 g of lithium chloride can cause fatal poisoning. Other lithium salts such as lithium carbonate are used in treatment of manic depression illness, however at concentrations above 1.2 meq/L lithium. Side effects may appear such as excessive urination, thirst, nausea and diarrhoea (McKetta, 1988). Lithium hydroxide has similar caustic properties to those of alkali-metal hydroxide. No industrial disease caused by ingestion of lithium compounds has been reported so far (Wietelmann and Bauer, 2003).

2.9 Conclusions from literature review

From the review it can be concluded that Zimbabwe has substantial lithium-containing mineral reserves. The lithium ore concentrate is exported without any further beneficiation. The products of beneficiation (lithium compounds) have much higher economic value compared to the concentrate. In addition the increase in the global market over the past years for lithium ion batteries could further increase the demand for the metal and/or its compounds. .

The sulphuric roasting process was chosen as subject for this study for the processing of the Zimbabwean petalite because of the merits associated with it, *viz.* high yields and relatively low energy requirements. In addition, sulphuric acid cheaper and is easier to handle and less aggressive compared to other acids such as HCl.

3 MATERIALS AND METHODS

3.1 Materials

Laboratory tests were carried out with a petalite concentrate, as received from Bikita Minerals (Pvt) Ltd in Zimbabwe. A multi-element standard (ICP grade) and analytical grades Na_2CO_3, H_2SO_4 (98 %), HCl (32 %), $CaCO_3$, HF (40 %) and $Ca(OH)_2$ from Merck Chemicals (Pty) Ltd were used. High purity carbon-dioxide (99.95 % minimum) gas from Afrox (Pty) Ltd was used. Distilled water was used in the preparation of all aqueous solutions.

3.2 Instrumentation

The following instruments were used in this study: for X-ray fluorescence (XRF) a Thermo ARL9400 XP instrument; for inductively coupled plasma optical emission spectrometry (ICP-OES) a SPECTRO ARCOS; for X-ray diffractometry (XRD) a PANalytical X'Pert PRO diffractometer; for mass measurements a Mettler PM2000MC balance; for pH measurements a pH meter Cripson GLP 21; for thermogravimetric analysis (TGA) a TA instrument DSC-TGA SDT Q600; for particle size distribution and specific area a particle size analyser a Malvern Mastersizer 2000; and for scanning electron microscopy (SEM) a Joel JSM-5800 LV. For technical details, see Appendices A.1 (XRD), A.2 (XRF), A.3 (SEM), A.4 (ICP-OES) and A.5 (TGA).

3.3 Methods

3.3.1 Particle size analysis

Particle size distribution of the petalite concentrate and its corresponding particle surface area were done using a laser particle size analyser using water as dispersant.

3.3.2 Characterisation of the concentrate

Elemental analysis of the concentrate was done using XRF and ICP-OES. The petalite sample was dissolved completely using a method adapted from Stoch (1986) to determine % Li_2O content. 0.5 g of petalite was decomposed by HF-H_2SO_4 followed by dissolution of soluble salts by boiling with water. XRD analysis was performed using Fe filtered Co K_α as a radiation source. The phases were identified using X'Pert Highscore Plus software. The semi-quantitative phase amounts (weight %) was estimated using the reference intensity method in the X'Pert Highscore Plus software.

3.3.3 Calcination and roasting of petalite

The finely powdered petalite concentrate was first heated in a laboratory furnace at 1100 ℃ for 2 hrs. Heating petalite to high tempera tures results in an irreversible phase change to a β-spodumene-SiO_2 solid solution which is more reactive to acid and base attack (Wietelmann and Bauer, 2003; Kamiensiki et al., 2005; Garrett, 2004). A weighed amount of ground pre-heated petalite sample was mixed with concentrated H_2SO_4 in a porcelain crucible. An amount of acid 15 % in excess of the lithium equivalent was added. The roasting temperatures were varied from 200-300 ℃. The mixture in a crucible was placed in a laboratory furnace when the desired temperature was attained. On completion of the roasting process the samples were removed, cooled at room temperature, and ground to less than 75 µm. The reaction of β-spodumene with H_2SO_4 is shown in equation (12) (Mcketta, 1988).

$$Li_2O.Al_2O_3.4SiO_2(s) + H_2SO_4(conc) \rightarrow Li_2SO_4(s) + Al_2O_3.4SiO_2(s) + H_2O(g) \quad (12)$$

3.3.4 Leaching studies

This study addresses conditions such as temperature, leaching time, solid/liquid ratio and stirring rate which affect leaching of lithium. Leaching experiments were performed in a 600 mL flat-bottomed pyrex glass beaker as a reactor. An accurately measured volume of distilled water was added to the reactor and heated to the desired temperature controlled at ±1 ℃ by a thermostatically controlled hot plate magnetic stirrer at atmospheric pressure. A PTFE coated stirring bar was used. When the temperature reached the pre-set value and remained stable, the acid roasted product was added to the reactor and heated together with the water. During leaching, samples were withdrawn at selected time intervals. After various leaching experiments had been conducted, ICP testing was done to calculate the extraction rate. To ensure reproducibility, leaching experiments were conducted in triplicate and reported values are the average of the three. The relative standard deviations were below 2.5 %.

3.3.5 Solution purification

Acid roasting and leaching of petalite concentrate is not entirely selective as co-dissolution of impurities also occurs. The resulting leach liquor contains aluminium, calcium, magnesium, iron and other impurities which can be removed by pH control and addition of a carbonate (Averill and Olson, 1977). $CaCO_3$ was added little by little to the acidic leach solution to obtain a pH of 3.8-6.5. At this pH Fe and Al were precipitated and the cake was filtered and washed with water. Mg was precipitated using $Ca(OH)_2$ and filtered. The filtrate was treated with Na_2CO_3 at 25 ℃ which produced a pH between 11-12. Na_2CO_3 equivalent to the amount of calcium present was added. This precipitated the Ca, which was removed by filtration. The flow sheet of the purification procedure is shown in Figure 7. A pH meter was used during the procedure for the pH value analysis. ICP-OES was used to determine the concentration of lithium and impurities at each stage. Reproducibility of the process was tested by running the experiments in triplicate. Errors for each were below 3 %. The purified solution was

adjusted to pH 7-8 using H_2SO_4 (1 mol L^{-1}) in order to precipitate the carbonate (Kamiensiki et al., 2005; Demirbas, 1999).

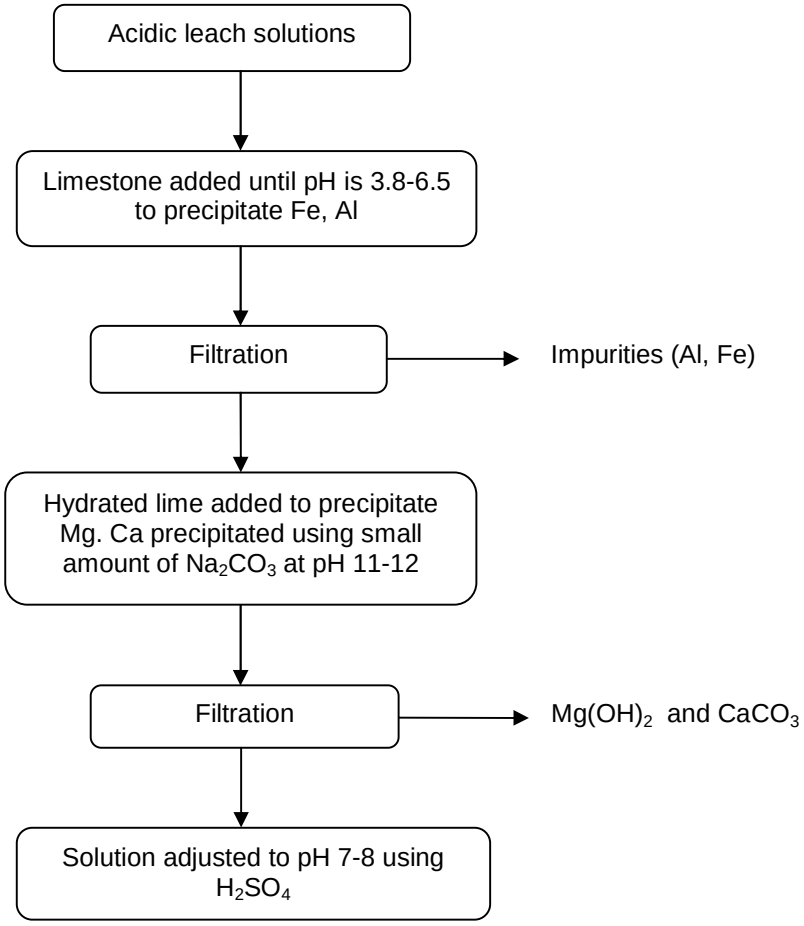

Figure 7. Flow sheet for leach liquor purification.

3.3.6 Precipitation of lithium from leach liquor

The purified leach solution was evaporated to about 50 % of its original volume and filtered to remove the calcium residue. The evaporation process was continued until the concentration of Li was more than 11 g L^{-1}. A hot saturated solution of Na_2CO_3 was added drop-wise to the filtrate at 95-100 ℃ giving a white precipitate of Li_2CO_3. The precipitate was filtered and washed thoroughly with water (95-100 ℃) to remove

residual Na_2SO_4 and excess Na_2CO_3. The water-washed Li_2CO_3 was dried at 250 ℃. The flow sheet for the lithium recovery procedure is shown in Figure 8. Changes of the lithium and impurity concentration during the processing of leach liquor were recorded by means of ICP. To ensure precision and repeatability of the process, experiments were run in triplicate. The relative standard deviations were less than 3.5 %. Na_2SO_4 in the mother liquor was crystallised by chilling the solution at 0-8 ℃ followed by pressure filtration (Garrett, 2004). The filtrate which contains some lithium and residual Na_2CO_3 was recycled to the evaporator.

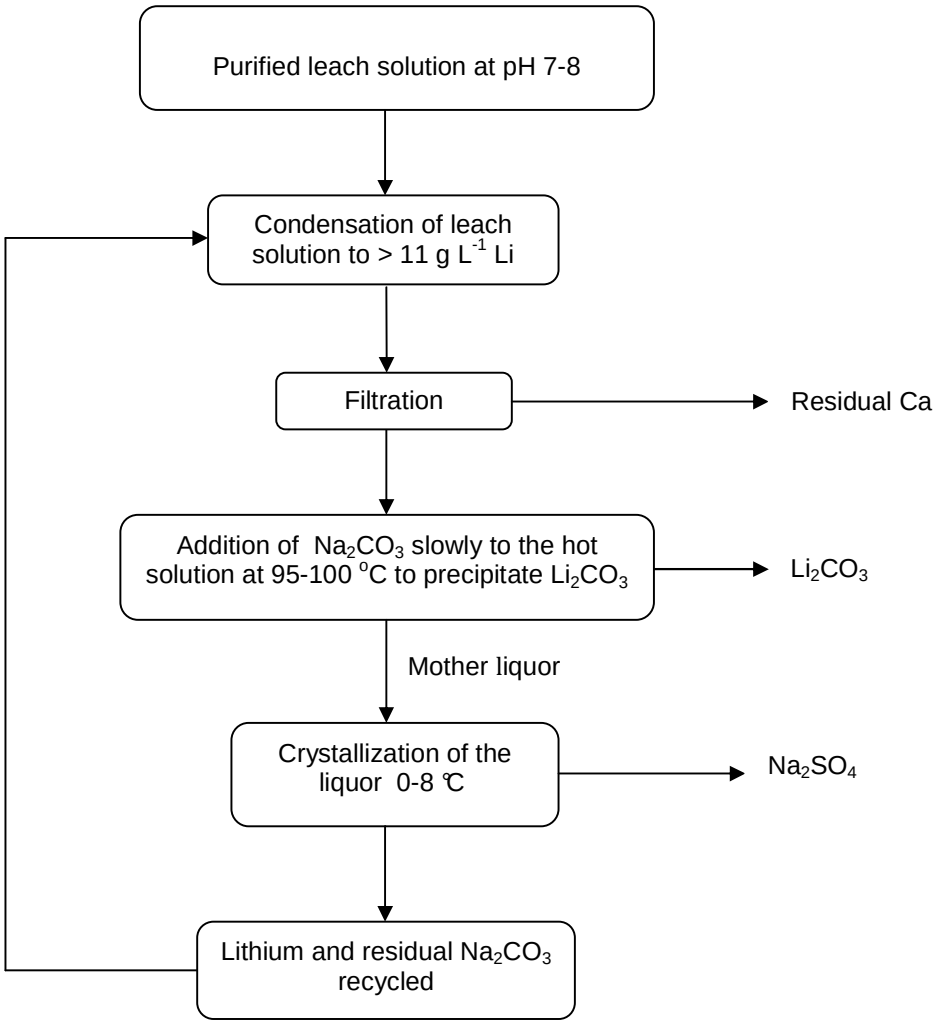

Figure 8. Flow sheet for precipitation of Li_2CO_3.

3.3.7 Characterisation of lithium carbonate

The dried Li_2CO_3 was subjected to phase, thermal and chemical analysis. Phase and thermal analysis was done by XRD and TGA respectively. XRD analysis was performed using X-ray diffractometer with Fe filtered Co K_α as a radiation source. During TGA investigations, samples of 10 ±1.5 mg were measured in a temperature range of 25-1090 ℃ at a rate of 10 ℃ min^{-1} in flowing N_2. Comparison was made for the synthesised and commercial Li_2CO_3 from Alfa Aesar, a Johnson Matthey Company. Chemical analysis was done by means of ICP to determine the purity of Li_2CO_3. 0.50 g of processed Li_2CO_3 was dissolved with concentrated HCl at 90 ℃ for 30 minutes (Wang et al., 2009) and made up to 100 mL with distilled water in a volumetric flask. The solution was subjected to ICP analysis to determine the lithium and impurity concentration. ICP analysis experiments were conducted in triplicates. The relative standard deviations were below 2 %.

3.3.8 Preparation of lithium fluoride

25.00 g of the synthesised lithium carbonate (0.3384 mol) was accurately weighed and mixed with distilled water to prepare a solution of 50 g L^{-1} Li_2CO_3. The mixture was then charged into a 2 L conical flask reactor vessel. The reactor temperature and stirring speed was controlled at 25 °C and 350 rpm respectively using a heating magnetic stirrer. High purity carbon dioxide (CO_2) was injected into the reactor at a pressure of 400 kPa with the CO_2 flow rate kept at 250 cc/minute. A reaction time of 1 hour 30 minutes was found enough to dissolve lithium carbonate completely. At the end of the experiment, the CO_2 flow was stopped and the solution was filtered to remove any residue present with Whatman filter paper number 1 using a venturi system. The reaction mechanism of the dissolution process is described fully in chapter 2.

The experimental set up for lithium carbonate dissolution is shown in figure 9.

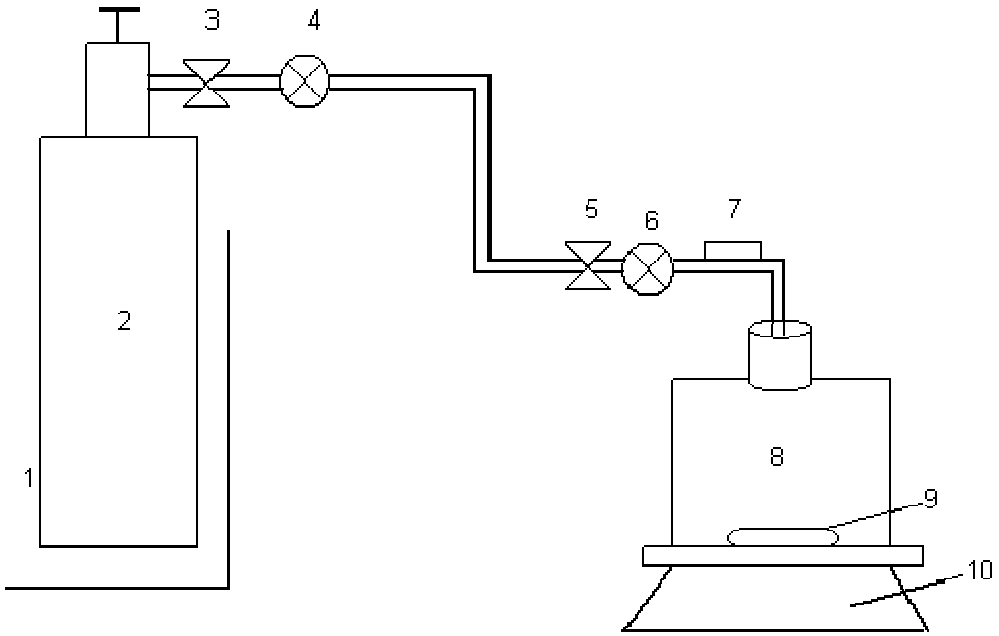

Figure 9. Schematic diagram of the experimental setup of Li_2CO_3 carbonation. (1) FMG cylinder store, (2) CO_2 gas cylinder, (3) Valve, (4) Pressure gauge, (5) Valve, (6) Pressure gauge, (7) Gas flow meter, (8) Conical flask reactor, (9) Stirring bar, (10) Magnetic stirrer.

25 mL of the dissolved solution (0.03384 mol Li_2CO_3) was admixed slowly with HF (40 %), 20 % in excess of the equivalent through the following reaction (13):

$$LiHCO_3(aq) + HF(aq) \rightarrow LiF(s) + H_2O(aq) + CO_2(g) \quad (13)$$

The precipitation reaction was carried out is a 250 mL PTFE beaker. Heating was done using a heating magnetic stirrer with teflon coated stirring bar. The precipitated LiF was filtered using a Whatman filter number 1 under the venturi system. The residue was washed with distilled water and dried completely at 250 °C for 1 hour. The dried LiF was weighed to determine the yield. The effect of precipitation parameters such as temperature, pH, concentration and stirring speed on the morphology and particle size of the precipitated particles was examined. For determination of the effect of

concentration on the precipitation process, two sample solutions of concentration 25 g L^{-1} and 50 g L^{-1} Li_2CO_3 were prepared. 25 g L^{-1} was prepared by diluting the 50 g L^{-1} lithium carbonate solution. HF was added at 20 % in excess of the equivalent amount. The effect of pH was determined by adding different amounts of HF solution more than the equivalent amount to the Li_2CO_3 solution. pH was recorded using Whatman pH paper strips.

The dried LiF was subjected to phase, morphology, specific surface area and laser particle size analysis using XRD, SEM and a laser particle size analyser respectively. Comparison was made between the synthesised and purchased LiF from Merck. For chemical analysis 0.50 g of the synthesised LiF powder was dissolved completely with HCl (32 %) at laboratory temperature and made up to 100 mL with distilled water in a volumetric flask. The solution was subjected to ICP analysis to determine the lithium and impurity concentration. To determine the yield of LiF and the reproducibility of the procedure, experiments were conducted in triplicate and the reported values are the mean values. The relative standard deviations were below 2.5 %.

3.3.9 Preparation of lithium chloride

Accurately-weighed, synthesised 2.5 g lithium carbonate was dissolved completely with HCl (32 %), 20 % in excess of the equivalent at 25 °C forming a solution of lithium chloride. A 250 mL PTFE beaker was used as reactor. Heating was done using a heating magnetic stirrer with PTFE coated stirring bar. The stirring speed was set at 350 rpm. The solution was neutralised to pH 5.0 by addition of lithium carbonate followed by filtration using a Whatman filter paper number 1 using a venturi system. The residue was recycled. The anhydrous powder was recovered from solution by evaporation in a brick lined oven at 250 ℃ to minimise contact of the product with moisture from the atmosphere.

The anhydrous lithium chloride was ground and subjected to phase and thermal analysis using XRD and DSC-TG respectively. Comparison was also made between the synthesised and commercial LiCl from Merck. For chemical analysis, 0.50 g of anhydrous LiCl was dissolved completely with water at 25 ℃ for 30 minutes and made up to 100 mL with distilled water in a volumetric flask. The solution was subjected to ICP analysis to determine the lithium and impurity concentration. ICP analysis experiments were conducted in triplicate and the mean values were reported. The relative standard deviations were below 2 %.

CHAPTER 4 RESULTS AND DISCUSSION

4.1 Particle size distribution

The particle size distribution of as-received petalite concentrate is shown on Figure 10. The particle size analyser indicates that the volume weighted particle size mean is 40.0 µm and a corresponding surface area of 0.6 m^2/g. Small mineral particle size enhances the leaching rate since larger surface area of the mineral particle is exposed to chemical attack. The influence of mineral particle size thus cannot be overlooked in hydrometallurgical treatment.

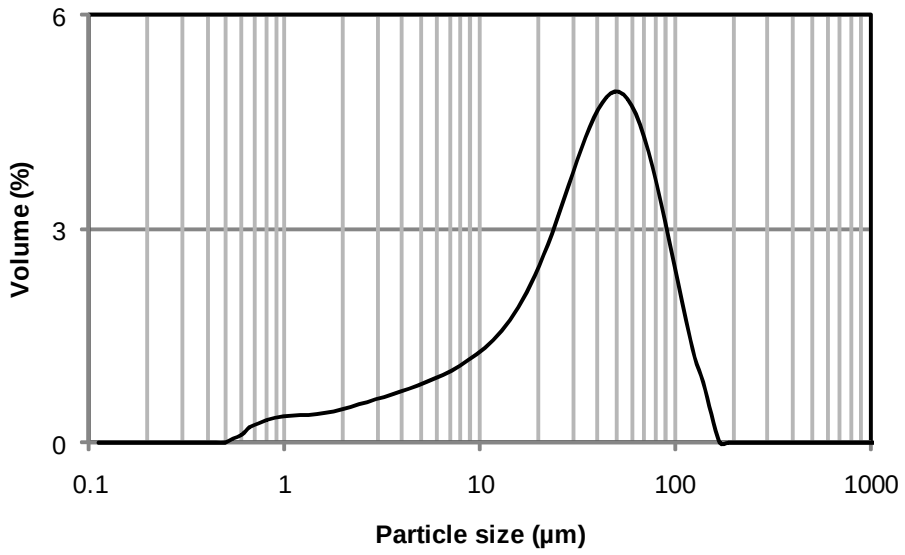

Figure 10. Particle size distribution of petalite concentrate.

4.2 Mineralogical composition of the concentrate

The mineral phases recorded from the XRD examination of the lithium pegmatite is provided in Table 8. XRD examination confirmed that the sample is a petalite. Furthermore the XRD data showed the presence of associated minerals, viz. spodumene, bikitaite, lepidolite, quartz, albite and microcline.

Table 8. Semi-quantitative mineral content of the petalite (XRD analysis).

Mineral phase	(Wt. %)
Petalite ($LiAlSi_4O_{10}$)	57.0
Spodumene ($LiAlSi_2O_6$)	3.0
Quartz (SiO_2)	4.0
Albite ($NaAlSi_3O_8$)	17.0
Bikitaite ($LiAlSi_2O_6(H_2O)$)	2.0
Lepidolite ($K(Al_{0.62}Li_{0.38})_2Li_{0.92}Si_4Al_{0.42}O_{10}(OH)_{0.485}F_{1.51}$)	10.0
Microline ($KAlSi_3O_8$)	7.0

4.3 Elemental analysis of the concentrate

The results of the XRF and ICP-OES showed Li_2O (4.10 %), SiO_2 (76.11 %) and Al_2O_3 (17.76 %) as major oxides. An earlier publication by Cooper (1964) on petalite from Bikita, Zimbabwe, showed similar results, Li_2O (4.36 %), SiO_2 (76.79 %) and Al_2O_3 (16.85 %). The chemical composition of petalite concentrate is shown on Table 9.

Table 9. Chemical composition of the petalite (XRF, ICP-OES analysis).

Component (%)	ICP-OES	XRF (Normalised)	Combined
SiO_2	-	79.37	76.11
Al_2O_3	-	18.52	17.76
Li_2O	4.10	-	4.10
Fe_2O_3	-	0.05	0.05
Na_2O	-	0.57	0.54
K_2O	-	0.47	0.45
CaO	-	0.12	0.11
Rb_2O	-	0.09	0.09
P_2O_5	-	0.03	0.03
Cs_2O	-	0.03	0.03
MnO	-	0.02	0.02
F	-	0.01	0.01
CeO_2	-	0.09	0.09
Cr_2O_3	-	0.00	0.00
MoO_3	-	0.01	0.01
LOI* (1000 ℃)		0.62	0.59
Total		100.00	100.00

* Loss on ignition

The XRF analysis is restricted to elements fluorine to uranium. Lithium is too light to be detected by XRF, and ICP-OES was employed to determine Li_2O content. The XRF results were combined with ICP-OES results shown in Table 9. Each combined mass percentage value (lithium oxide excluded) is calculated by normalizing the full XRF column to 95.9 %, i.e. 100 % – 4.1 %.

4.4 Roasting studies

4.4.1 Effect of roasting temperature and time

A number of experiments were run by varying the roasting temperature in the range of 200-300 ^{o}C. The results of this investigation are presented in Figure 11. An increase in temperature from 200 to 300 ^{o}C brings about an increase in dissolution of lithium, which is attributed to the fact that raising the temperature will increase the reaction rate. From the graph optimal extraction was achieved at 300 ℃ in 60 minutes. This corresponds to 97.3 %. The remaining % is stuck in the residue as there is no leaching process which is practically 100 % efficient. Garrett (2004) reported comparable results with lithium extraction efficiency of 97 % using 50 % excess sulphuric acid, roasting at 250 °C using a Canadian spodumene concentrate. However, much lower lithium extraction of 85 % was reported by Jandová et al. (2010) on zinnwaldite from Czech Republic using alkaline digestion method.

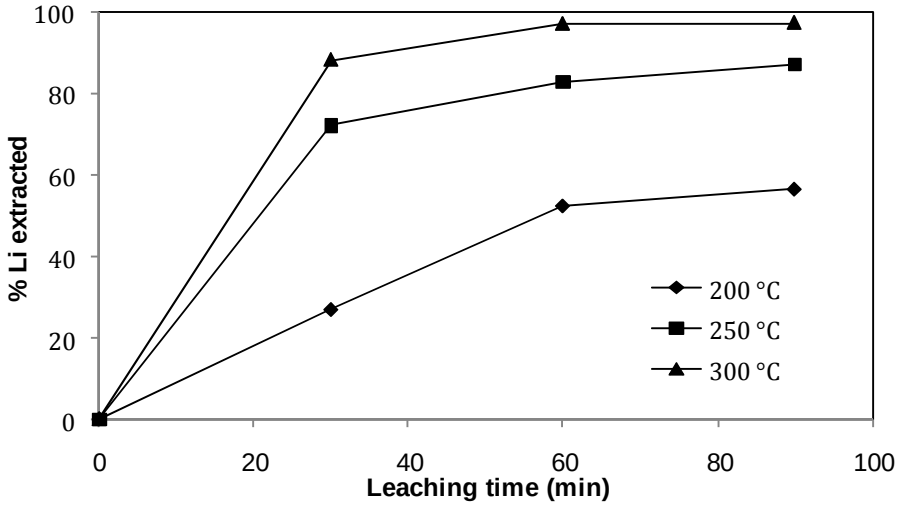

Figure 11. Effect of roasting temperature on the extraction rate of lithium. Experimental conditions: leaching temperature 50 ℃, leaching time 60 minute s, stirring speed 320 rpm and solid/liquid ratio (1/7.5 g/mL).

4.5 Leaching studies

4.5.1 Effect of stirring rate

The effect of agitation on the dissolution of lithium was investigated in water at 50 ^{o}C, using stirring speeds of 0-400 rpm with a solid/liquid ratio of (1/7.5 g/mL). The results in Figure 12 show that stirring speed has a significant effect on the dissolution of lithium. Agitation is required to keep the solids in suspension as well as to exclude the influence of external mass transfer (diffusion through liquid boundary layer). Above 320 rpm, the stirring rate no longer influences the lithium dissolution. On the basis of the data, subsequent experiments were carried out at a stirring speed of 320 rpm.

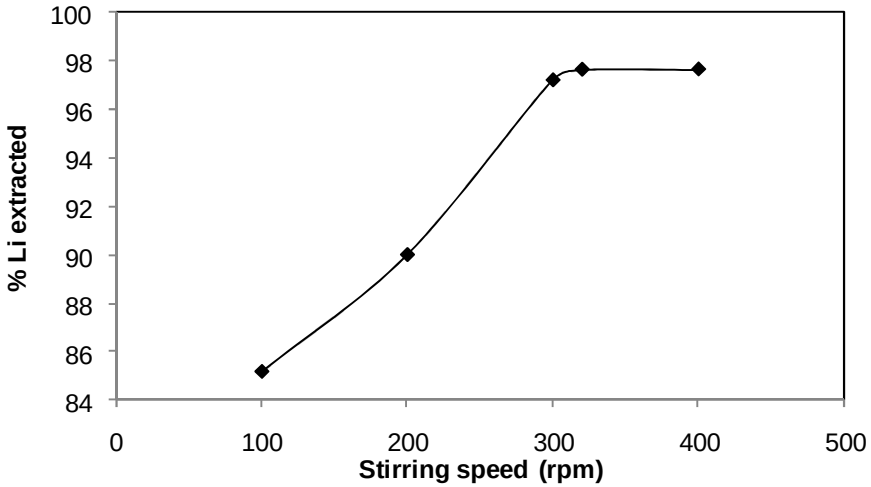

Figure 12. Effect of stirring speed on the extraction rate of lithium. Experimental conditions: acid roasting temperature 300 ^{o}C, acid roasting time 60 minutes, leaching temperature 50 ℃, leaching time 60 minutes and solid/liquid ratio (1/7.5 g/mL).

4.5.2 Effect of solid/liquid ratio

The effect of solid-to-liquid (g/mL) ratio was also examined. The results of different solid to liquid ratios are illustrated on Figure 13. It can be seen from Figure 11 that the percentage lithium extracted decreases with increasing solid-to-liquid ratio. A decrease in solid-to-liquid ratio decreases the viscosity of the system and as a result decreases

the mass transfer resistance in liquid-solid interface. From figure 13, at higher solid to liquid ratios the leaching agent was not stoichiometrically sufficient completely dissolve the lithium. The solid to liquid ratio of (1/7.5 g/mL) gave the highest dissolution and was kept for further use in this study. Jandová et al. (2010) reported an optimum solid-to-liquid ratio of (1/10 g/mL), when leaching calcines, obtained by alkaline roasting of zinnwaldite, with water.

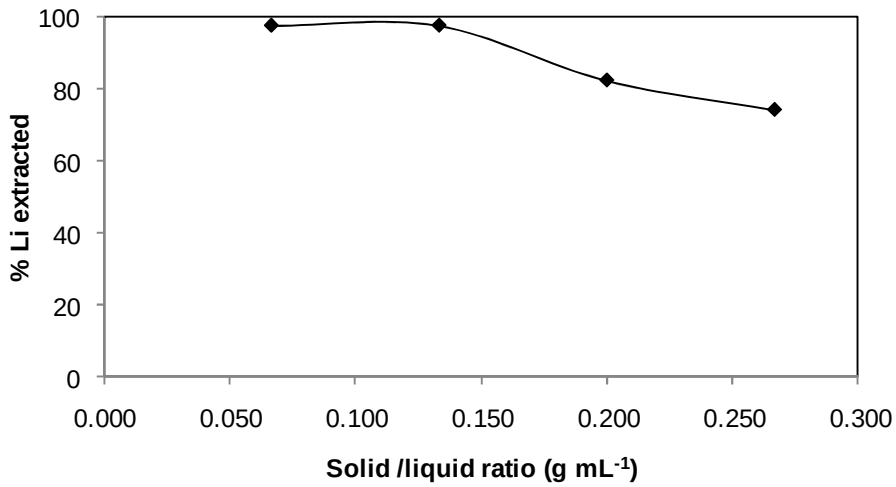

Figure 13. Effect of solid/liquid ratio on the extraction rate of lithium. Experimental conditions: acid roasting temperature 300 ^{o}C, acid roasting time 60 minutes, leaching temperature 50 ℃, leaching time 60 minutes and stirring speed 320 rpm.

4.5.3 Effect of leaching temperature and time

The effect of temperature on the dissolution of lithium was investigated with solid/liquid ratio of (1/7.5 g/mL) stirring speed of 320 rpm at temperatures 50 and 90 ^{o}C. From the results in Figure 14, it can be shown that temperature has very little effect on the extraction of lithium. The highest extraction of around 97.30 % was realised after 60 minutes for all the temperatures. To avoid significant loses of liquid by evaporation the temperature of 50 ^{o}C was used for subsequent experiments. Garrett (2004) also reported that leaching temperature has little effect on lithium dissolution. Acceptable

results were obtained at room temperature. Kondás and Jandová (2006) reported leaching times of 10 minutes at 90 °C on sinters obtained from processing zinnwaldite, using the gypsum process.

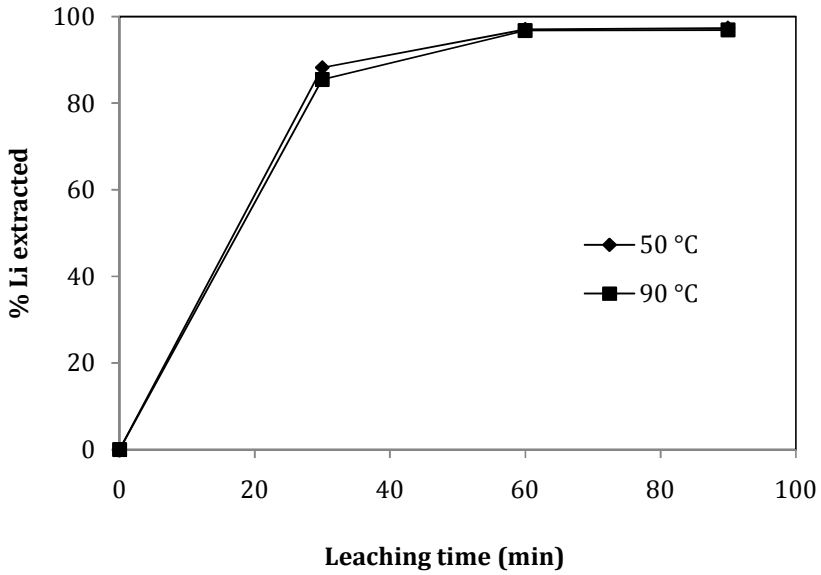

Figure 14. Effect of leaching temperature on the extraction rate of lithium. Experimental conditions: acid roasting temperature 300 ^{o}C, acid roasting time 60 minutes, stirring speed 320 rpm, leaching time 60 minutes and solid/liquid ratio (1/7.5 g/mL).

4.6 Solution purification

Changes of lithium and impurity concentration during processing leach liquors are described in Table 10. It is indicated from the table that $CaCO_3$ is effective in removing Al and Fe by precipitation. The same implies to precipitation of Mg and Ca with $Ca(OH)_2$ and Na_2CO_3 respectively. A lithium yield of 92.36 % relative to the original leach liquor was recorded before concentration of the leach liquor.

Table 10. Concentration of elements in processed solutions.

Solution	pH	Elemental concentration (mg L^{-1})							
		Li	Ca	K	Na	Al	Si	Fe	Mg
Original leach liquor	0.95	5716.82	145.14	451.60	1422.70	10.05	33.21	37.95	12.24
Leach liquor on addition of ($CaCO_3$ and $Ca(OH)_2$)	10.25	5500.72	559.50	147.80	1015.30	<0.025	<0.01	<0.01	<0.01
Leach liquor on addition of (Na_2CO_3)	11.56	5227.65	11.36	131.90	2163.30	<0.025	<0.01	<0.01	<0.01
Concentrated leach liquor	8.00	11998.62	7.29	492.93	5362.32	0.04	<0.01	<0.01	<0.01
Mother liquor (filtrate)		1120.15							

4.7 Precipitation and characterisation of lithium carbonate

Precipitation of Li_2CO_3 was done at 95-100 ℃ because the solubility of li thium carbonate decreases with increasing temperature (Wietelmann and Bauer, 2003). Lagos and Becerra (2005) reported that precipitation with sodium carbonate is the most effective since sodium sulphate that also precipitates is eliminated by washing with hot water. Lithium carbonate is precipitated from an aqueous lithium solution using Na_2CO_3 according to the following reaction (14):

$$Li_2SO_4(aq) + Na_2CO_3(aq) \rightarrow Li_2CO_3(s) + Na_2SO_4(aq) \quad (14)$$

Analytical results show about 86.00 % of the lithium was recovered as a precipitate relative to the concentrated leach liquor. The results were comparable to those of Jandova et al. (2009) who reported a total efficiency of Li_2CO_3 precipitation from leach liquours of about 73 % with a purity of 99 % using K_2CO_3. Lagos and Bacerra (2005) also reported an average yield of 83 % during precipitation of lithium carbonate from

lithium chloride leach solution using Na_2CO_3. A lower yield might be due to NaCl formed which is reported to decrease the solubility of Li_2CO_3 (Burkert et al., 1970).

The thermogram for both synthesized and commercial Li_2CO_3 is shown in Figure 15. The thermogravimetric curve for the synthesised Li_2CO_3 is almost similar to that of commercial powder. Both thermograms show that below 700 ℃ the curves are smooth and the mass changed very little. At about 725 ℃ Li_2CO_3 starts to decompose releasing CO_2 according to the following reaction (15):

$$Li_2CO_3 \rightarrow Li_2O + CO_2 \quad (15)$$

Mass losses of 58.43 % and 60.83 % for synthesised and commercial Li_2CO_3 respectively were recorded. These correspond well to the expected stoichiometric mass loss of 59.55 %.

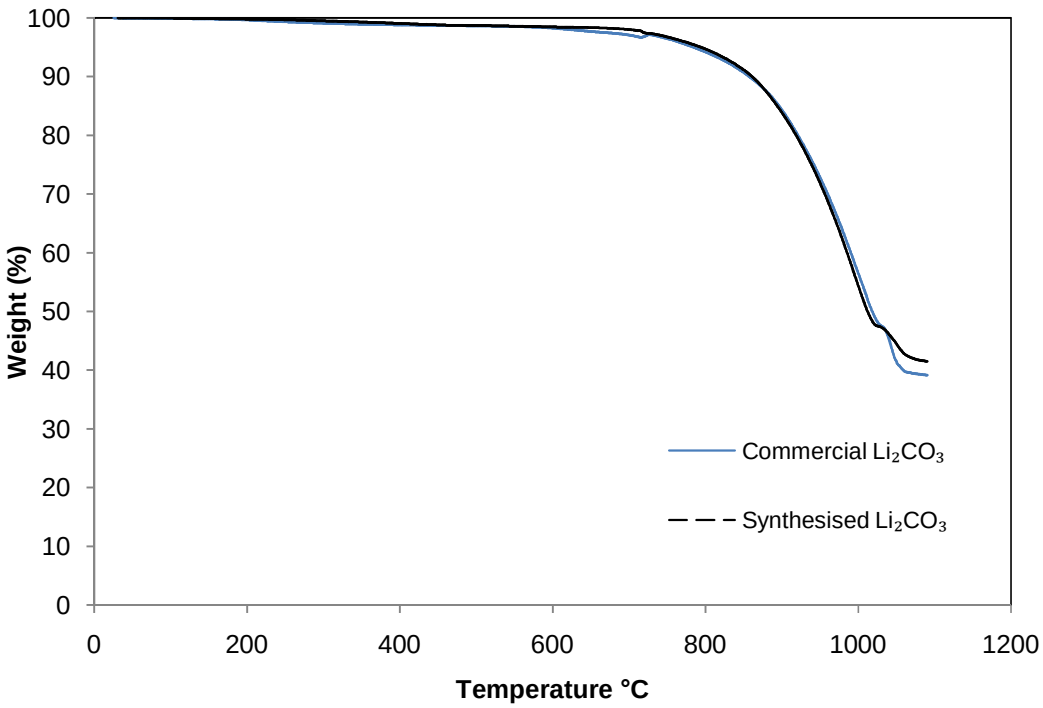

Figure 15. Thermograms of synthesised and commercial Li_2CO_3

A comparison between the X-ray diffraction pattern for synthesised and commercial Li_2CO_3 powder is shown in Figure 16. As can be seen, the XRD patterns for the synthesised and commercial powder are very similar. The results also indicate that no other phases were identified except the lithium carbonate. A slightly difference in peak intensities might be due to the difference in concentration of the powders.

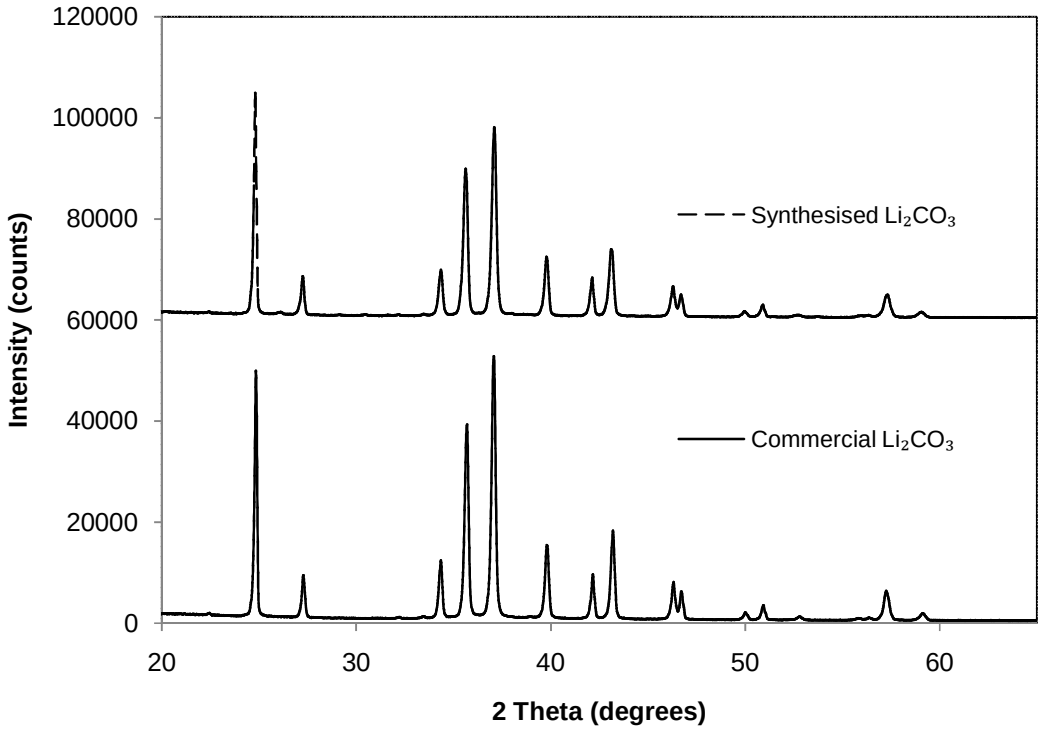

Figure 16. X-ray patterns of synthesised and commercial Li_2CO_3.

The purity of the synthesised product is indicated in Table 11. From the results, the purity of the recovered powder is 99.21 % (metal basis). The analysis shows that the major impurity is Na which may be attributed to the residual Na_2SO_4 and excess Na_2CO_3 that were not removed completely during the washing process.

Table 11. Content of impurities in lithium carbonate.

Li_2CO_3 purity (%)	Content of major impurities (wt %)						
	Ca	K	Na	Al	Si	Fe	Mg
99.21	<0.01	0.030	0.760	<0.01	<0.01	<0.01	<0.01

Figure 17 shows the particle size distribution of the synthesised Li_2CO_3. The volume weighted particle size mean of the synthesised powder is 1.4 µm with the corresponding surface area of 5.3 m^2/ g.

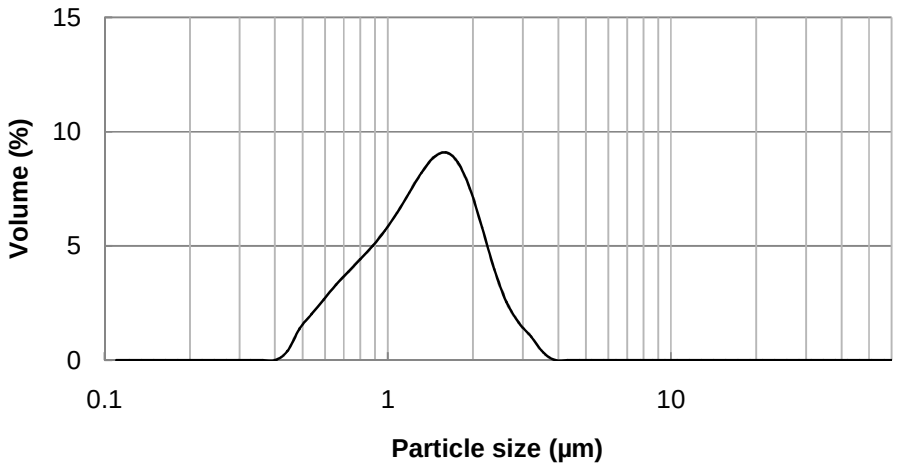

.

Figure 17. Particle size distribution of the synthesised Li_2CO_3 powder.

4.8 Precipitation of lithium fluoride

4.8.1 Effect of temperature

The effect of temperature on the morphology of particles was examined at 25 and 80 ℃. At 80 ℃ the dissolved lithium carbonate starts to re-precipitate out again before addition of HF according to reaction (15):

$$2LiHCO_3(aq) \rightarrow Li_2CO_3(s) + H_2O(aq) + CO_2(g) \quad (15)$$

At 25 °C LiF powder with cubic morphology was formed as depicted on Figure 18. On the basis of these results a temperature of 25 ℃ was chosen for subsequent experiments.

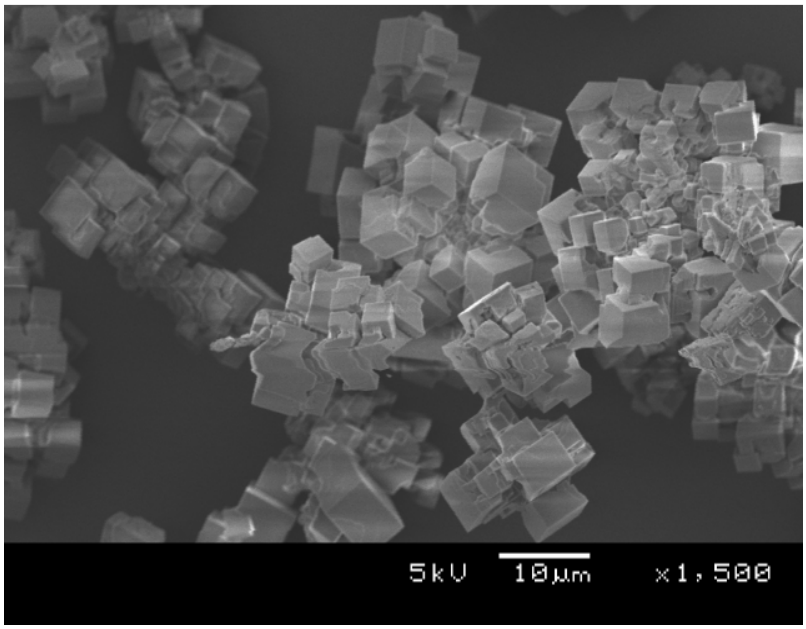

Figure 18. SEM images of LiF powder prepared at 25 °C.

4.8.2 Effect of pH

The effect of pH on the morphology of the precipitated particles is shown on figure 19, 20 and 21. As can be seen finer particles were produced at lower pH values. Sarraf-Mamoory et al. (2007) reported a similar trend when precipitating LiF from LiOH solution. Reduction of pH by adding higher amounts of hydrofluoric acid forces the reaction (13) to go to the right hand side according to the *Le Chatelier's* principle. A reduction in pH has a significant increase in nucleation rate resulting in finer particles produced at lower pH values. However, at pH 1.0 the particles become very small and highly agglomerated as indicated in Figure 19.

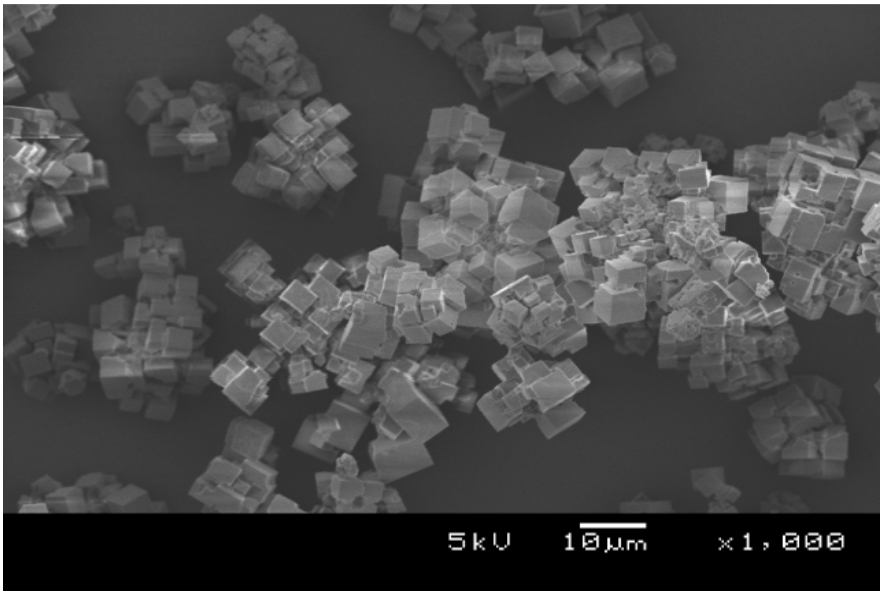

Figure 19. SEM images of LiF at pH 5.0.

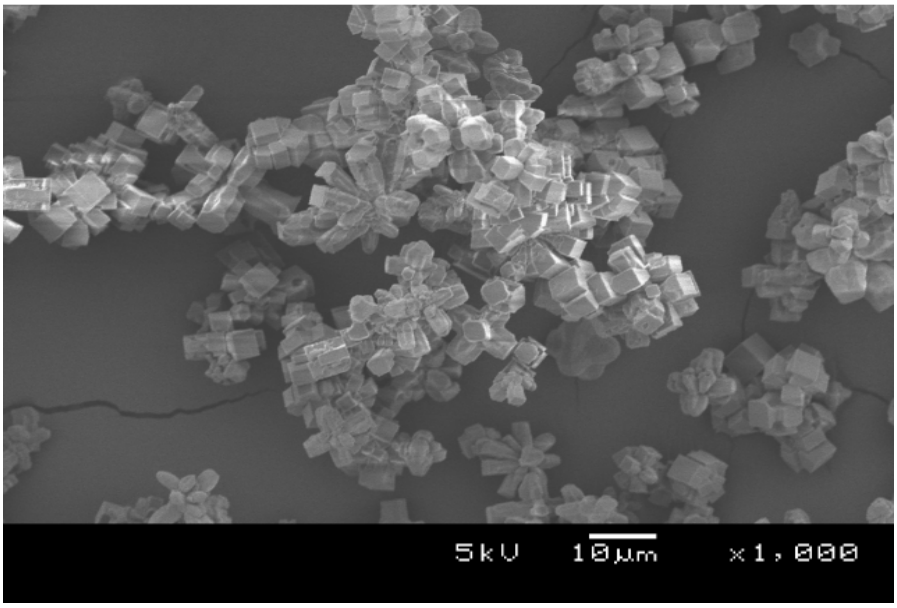

Figure 20. SEM images of LiF at pH 2.5.

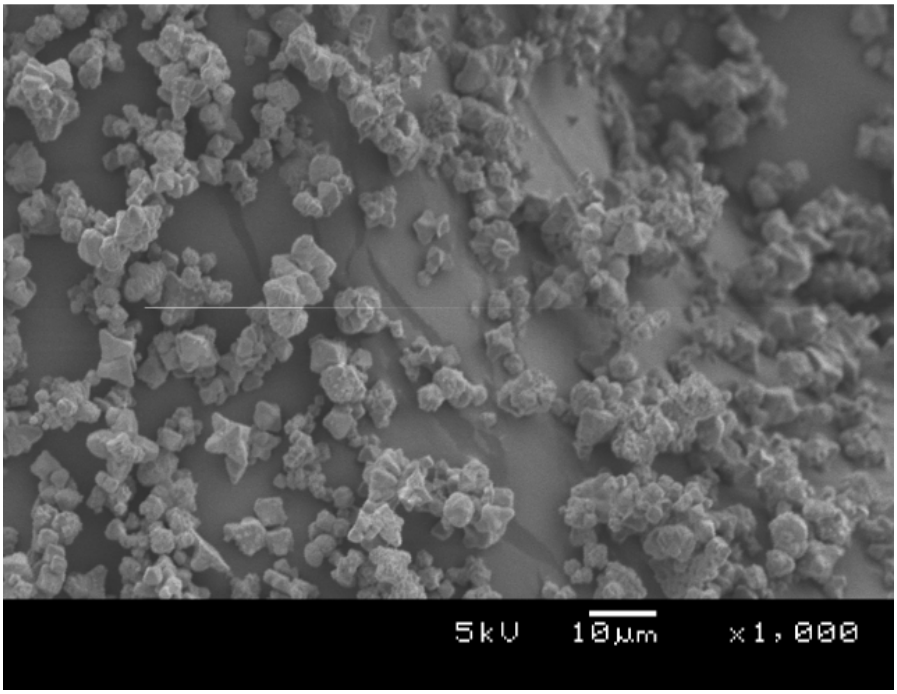

Figure 21. SEM images of LiF at pH 1.0.

4.8.3 Effect of concentration

The effect of concentration on the precipitation process was examined by preparing two solutions of concentration of 25 g L^{-1} and 50 g L^{-1} Li_2CO_3. HF was added at 20 % excess to the equivalent amount. The stirring speed and temperature were kept at 350 rpm and 25 °C respectively. From figure 22 and 23 it is clear that finer size distribution results at higher concentration of the starting solution. Increasing concentration increases the nucleation rate by increasing the number of nucleation sites.

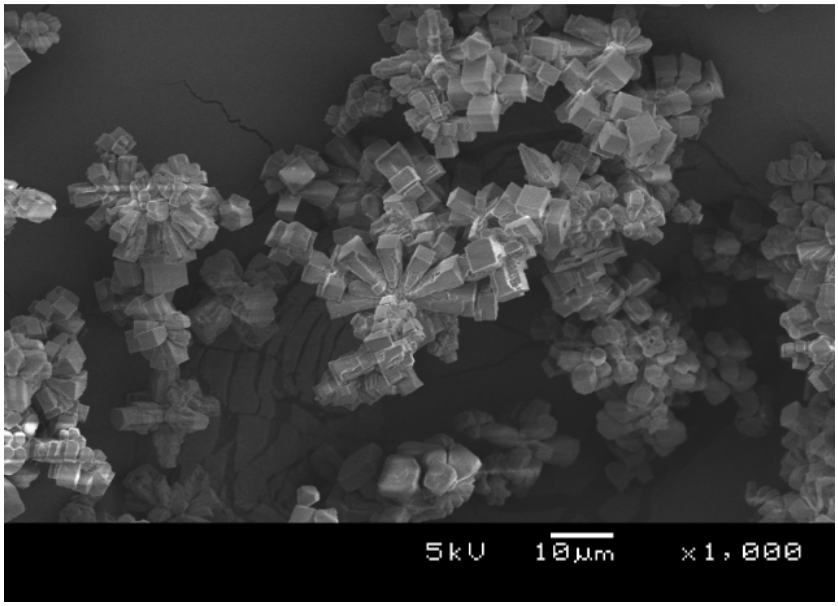

Figure 22. SEM images of LiF (25 g L^{-1} Li_2CO_3 solution).

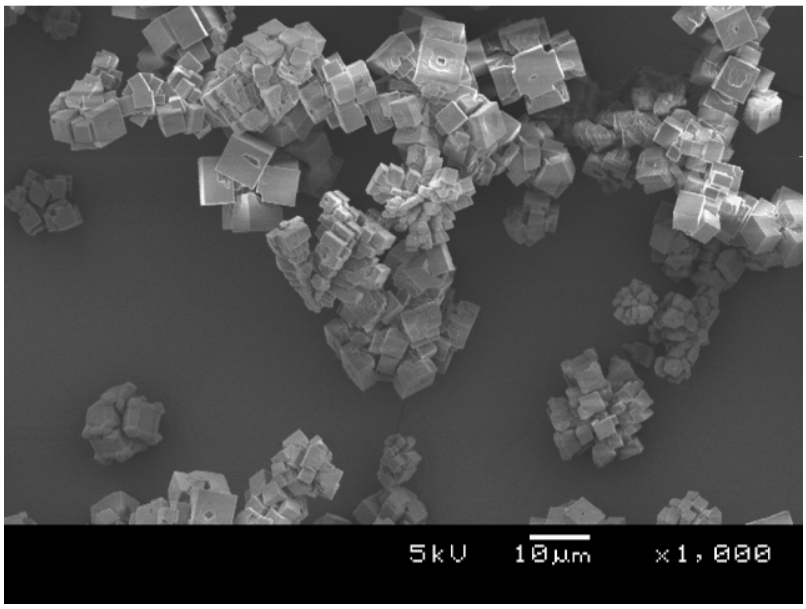

Figure 23. SEM images of LiF (50 g L^{-1} Li_2CO_3 solution).

4.8.4 Effect of stirring

The effect of stirring on the particles formed was examined at 0 and 350 rpm. Concentration of the lithium carbonate solution and temperature at 50 g L^{-1} and 25 °C respectively. As can be seen on figure 24 and 25, agitation of solution by magnetic stirrer results in less agglomerated particles.

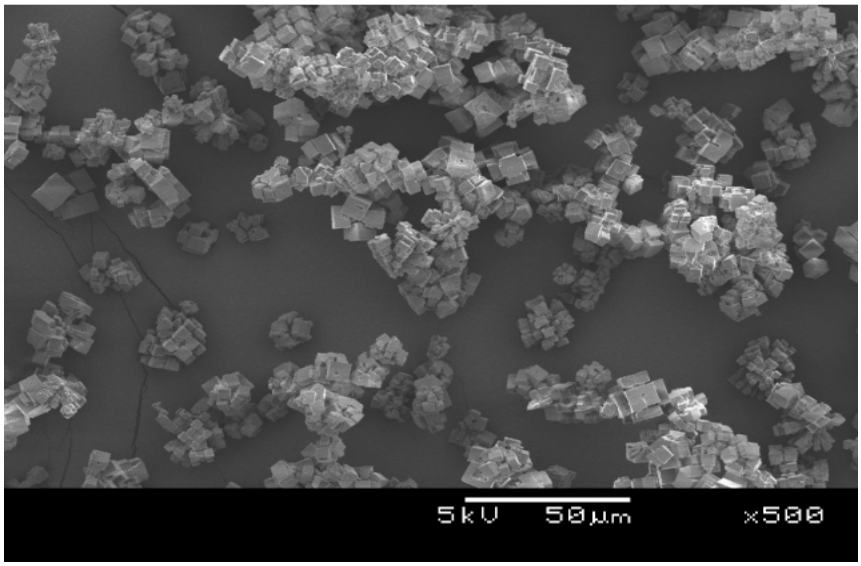

Figure 24. SEM images of LiF at 350 rpm.

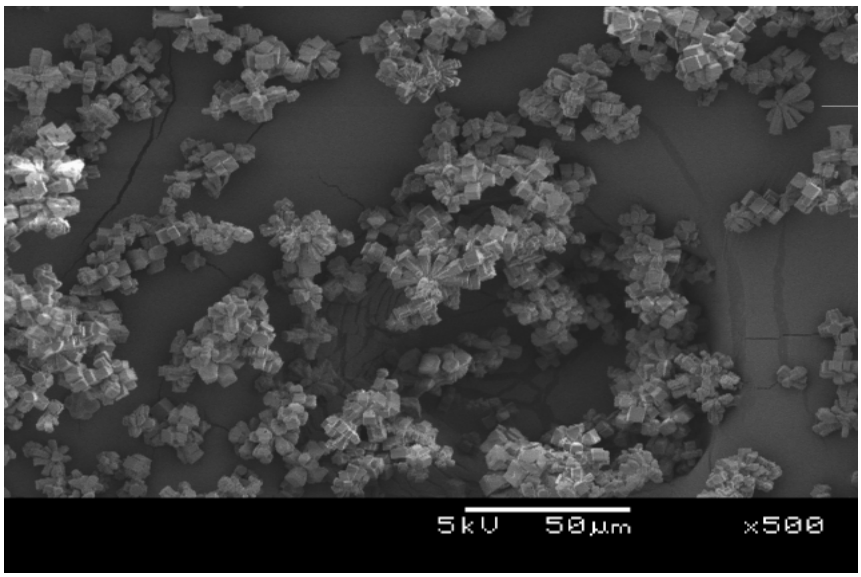

Figure 25. SEM images of LiF at 0 rpm.

4.9 Characterisation of LiF

Comparisons between XRD patterns and SEM images of the synthesised and purchased LiF from Merck are shown in Figures 26 and 27 respectively. As can be seen, the XRD patterns for the synthesised and purchased powder are very similar. XRD pattern indicates that no other phases are present except griceite (LiF). The synthesised powder and purchased powder have similar cubic morphology, in agreement with the literature (David, 2009; Kamiensiki et al., 2005). The purity of the recovered powder is 99.36 % as indicated on table 12. The major impurity is Na which may be attributed to the residual Na_2SO_4 and excess Na_2CO_3 that were not removed completely during Li_2CO_3 precipitation.

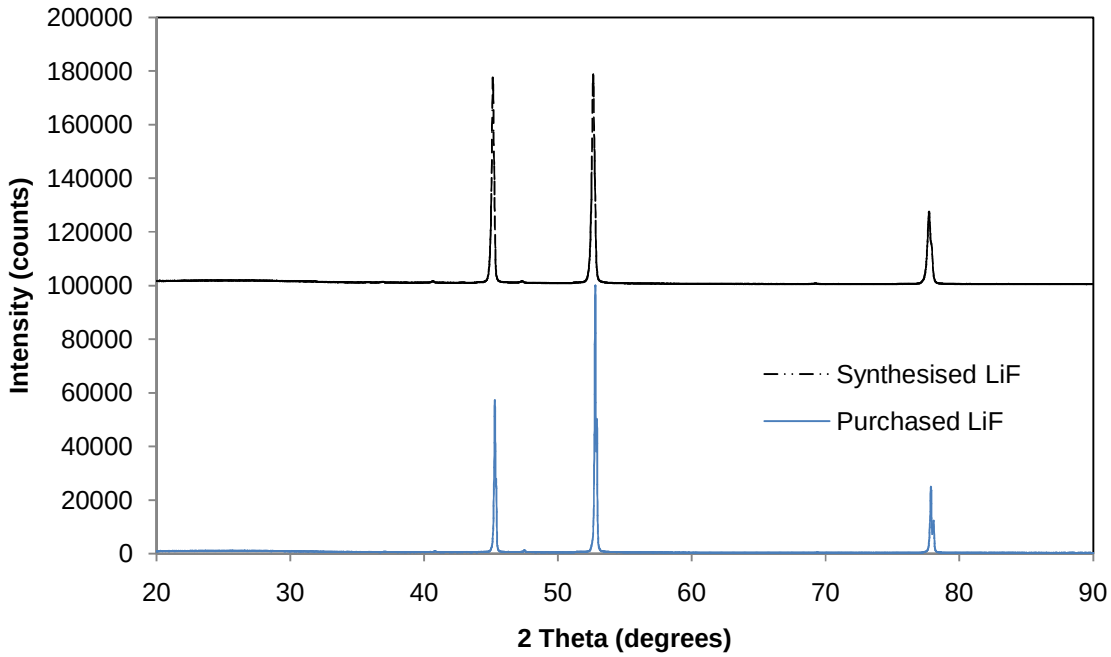

Figure 26. X-ray diffractogram of the synthesised and purchased Merck LiF.

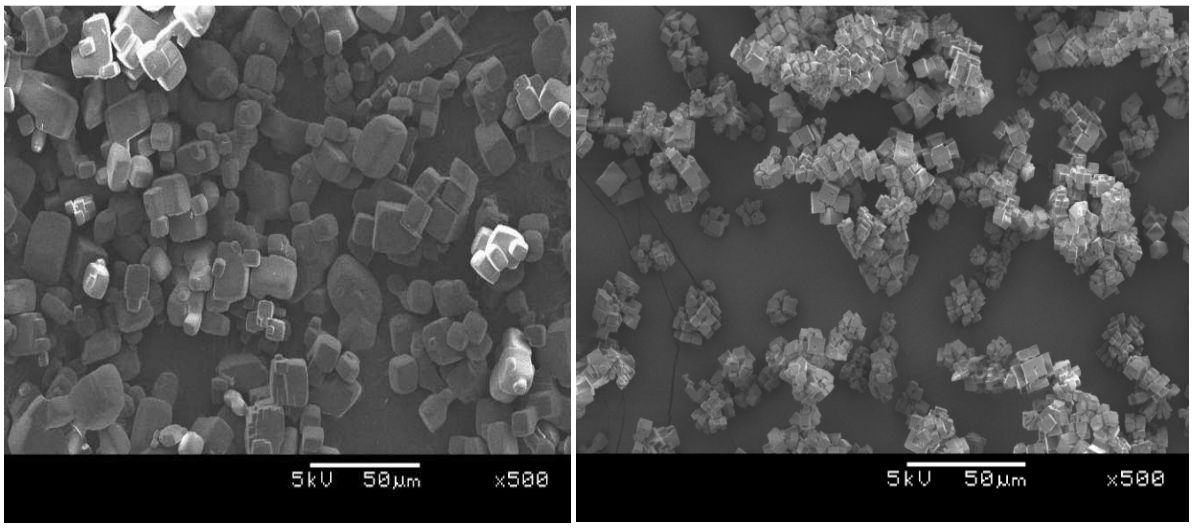

(a) (b)

Figure 27. (a) Commercial and (b) synthesised LiF powder.

Table 12. Contents of impurity in synthesised lithium fluoride.

LiF purity (%)	Content of major impurities (wt. %)						
	Ca	K	Na	Al	Si	Fe	Mg
99.36	0.01	0.02	0.47	<0.01	<0.01	<0.01	<0.01

The dried LiF was weighed and a yield of 96.53 % based on the amount of lithium carbonate used was determined. Friedrich (1999), reported a 95.5 % lithium fluoride precipitation efficiency using an almost similar method. The particle size distribution of the synthesised LiF using 20 % excess HF, a stirring speed of 350 rpm and 50 g L^{-1} Li_2CO_3 solution is shown on figure 28. The volume weighted particle size mean is 11.6 µm with the corresponding surface area of 0.2 m^2/g.

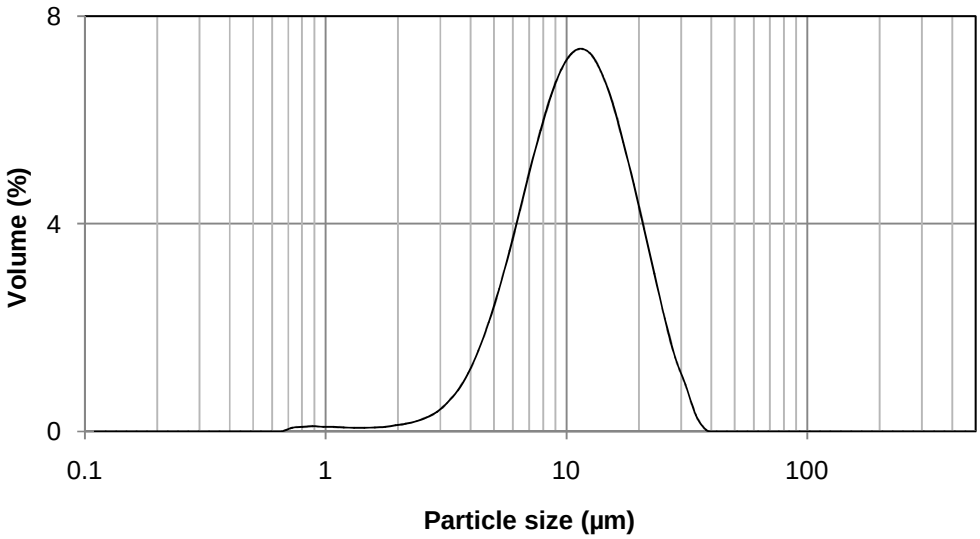

Figure 28. Particle size distribution of synthesised LiF.

4.10 Characterisation of lithium chloride

Characterisation of synthesised lithium chloride was done using XRD for phase analysis, DSC-TG for thermal analysis and ICP-OES for purity analysis. From the results of XRD on figure 29 it is clear that anhydrous LiCl particles can readily absorb water from the ambient atmosphere to form a surface layer of lithium monohydrate, $LiCl.H_2O$. It is also clear that anhydrous LiCl is the predominant component in the synthesised product with minor amount of monohydrate $LiCl.H_2O$. These results are in agreement with the phase data on table 6 which shows that $LiCl.H_2O$ is the first hydrate to form when LiCl is exposed to ambient atmosphere. It was also observed that when LiCl is exposed to air for a long period, the powder becomes wet on the surface and eventually turns liquid. Kamali et al. (2011) also reported similar observations.

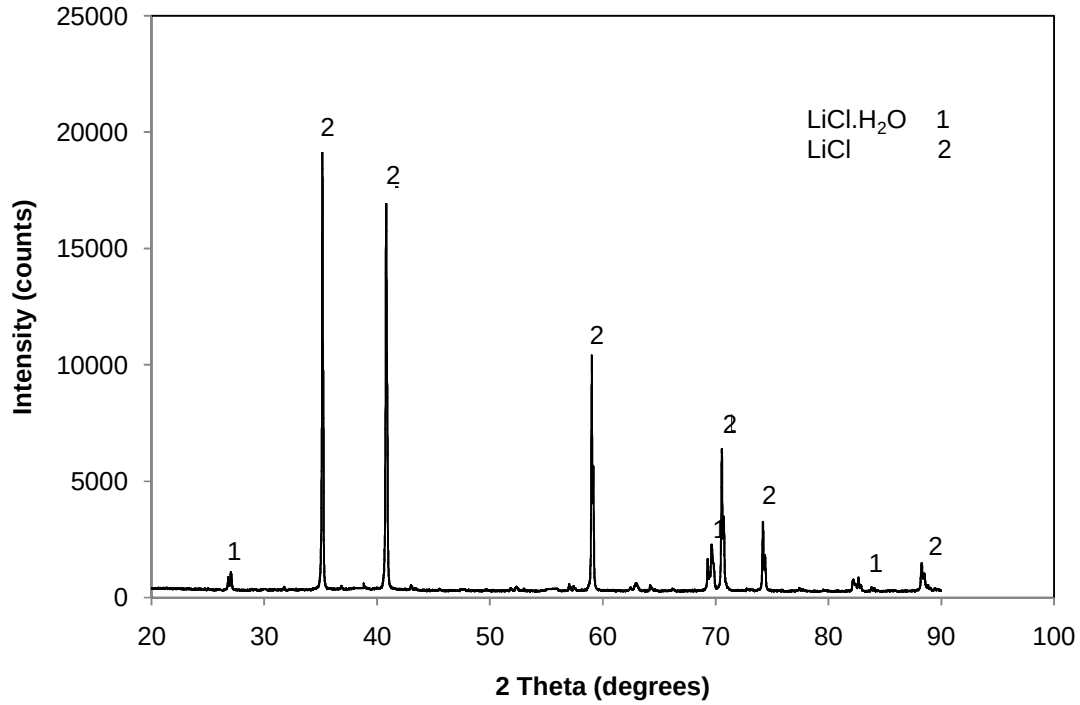

Figure 29. X-ray diffractogram of the synthesised LiCl.

For DSC-TG investigations, samples were measured in the temperature range of 18-1200 ℃ at a heating rate of 10 ℃ min $^{-1}$ in flowing N_2 at 50 mL min^{-1}. Alumina crucibles were used. The results for the DSC-TG for Merck and synthesised are almost identical and are displayed in Figure 30 and 31 respectively. The first mass loss for the synthesised LiCl occurs at temperature of around 104.8 °C which corresponds to the first peak on the graph and is attributed to the surface dehydration of the LiCl. This process was accompanied by a mass reduction of 1.8 %. From the DSC-TG graphs, at temperatures of 606.2 °C and 605.9 °C for synthesised and commercial products respectively the LiCl starts to melt. Integrating the area under these peak using the TA universal software, gives 19.8 kJ mol^{-1} and 18.4 kJ mol^{-1} the enthalpy of fusion for purchased and synthesised LiCl respectively. This information is presented in Appendix B. The values for melting point and enthalpy of fusion correspond well with 610.0 °C and 19.8 kJ/mol reported in the literature (David, 2009). At temperatures in excess of

the melting point, evaporation of LiCl occurs accompanied by extensive or heavy mass loss. The endothermic peaks occurring between 800 °C around 900 °C for both products is caused by the hydrolysis of LiCl to LiOH according equation (16)

$$LiCl + H_2O \rightarrow LiOH + HCl \quad (16)$$

At 992.8 °C, 98.8 % of LiCl had evaporated for synthesised LiCl and for purchased Merck LiCl, almost all the LiCl evaporated at 1030 °C. Evaporation for both synthesised and Merck LiCl took place at temperatures below the nominal boiling point of LiCl of 1382 °C. Kamali et al.(2011) also reported similar results.

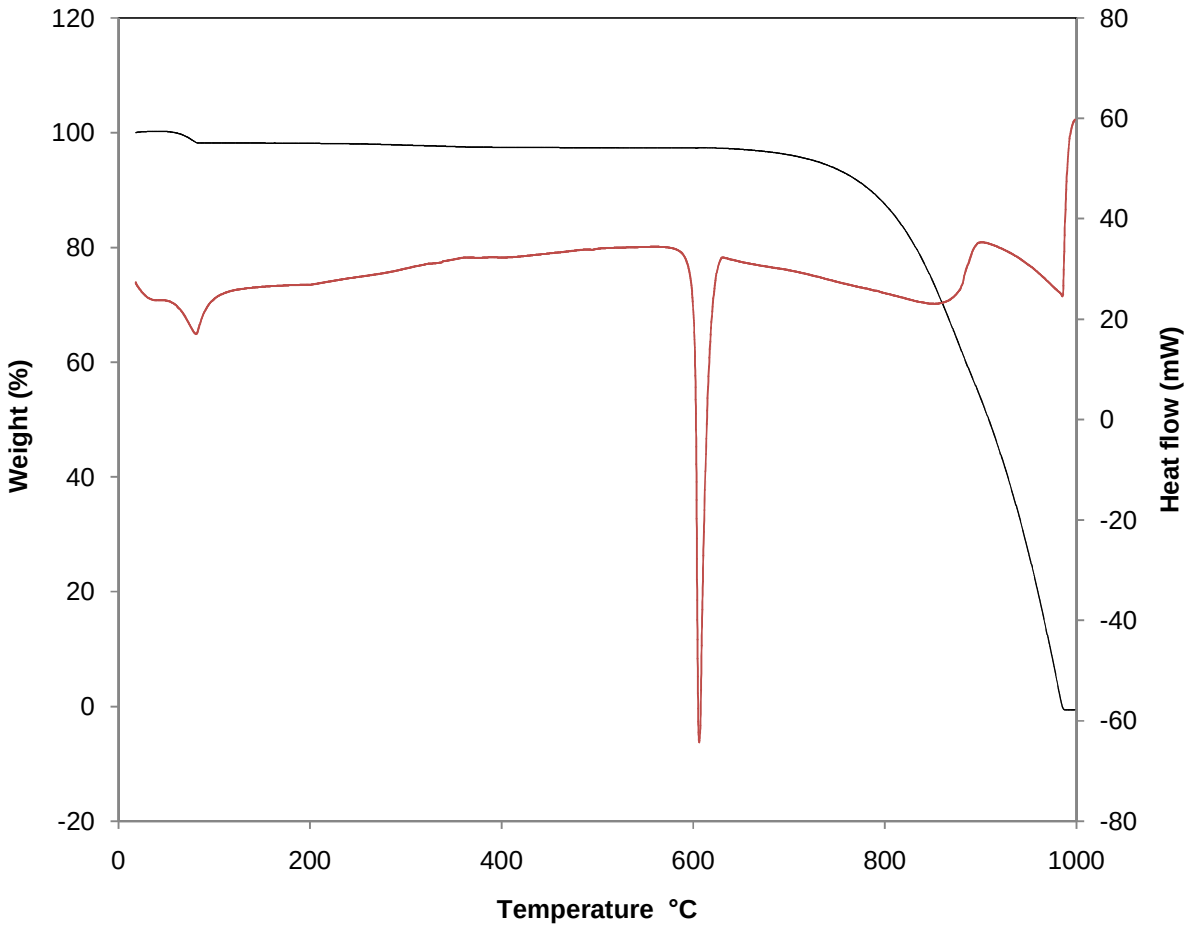

Figure 30. DSC-TG curves for synthesised LiCl.

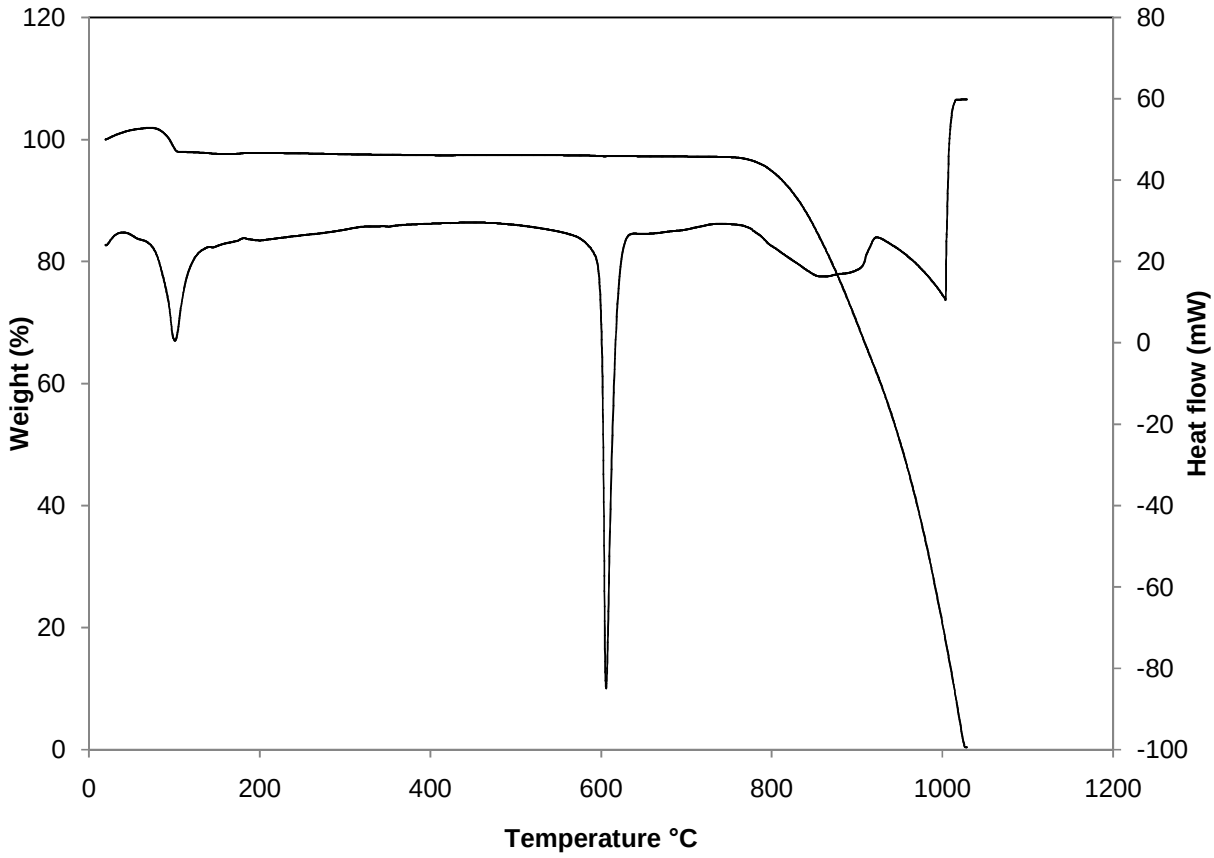

Figure 31. DSC-TG curves for purchased LiCl.

The purity of the recovered LiCl is 99.02 % as indicated on table 13. As in LiF, the major impurity is also Na which may be attributed to the residual Na_2SO_4 and excess Na_2CO_3 that were not removed completely during Li_2CO_3 precipitation.

Table 13. Contents of impurity in snythesised lithium chloride.

LiCl purity (%)	Content of major impurities (wt. %)						
	Ca	K	Na	Al	Si	Fe	Mg
99.02	0.02	0.051	0.62	0.06	<0.01	<0.01	<0.01

CHAPTER 5 CONCLUSIONS AND RECOMMENDATIONS

5.1 Conclusions

The study has demonstrated that it is possible to synthesise high economic-value products from the Zimbabwean petalite. Based on the experimental results the following conclusions were drawn.

The XRF and ICP-OES technique showed that the petalite concentrate has an average Li_2O content of 4.10 %. XRD examination on the other hand confirmed that the predominant mineral is petalite. It also revealed that presence of associated minerals, viz. spodumene, lepidolite, bikitaite, quartz, albitite and microline. The extraction rates of lithium are significantly influenced by roasting temperature, stirring speed and solid/liquid ratio. Maximum extraction of 97.30 % was realised at a roasting temperature of 300 ℃, solid/liquid ratio (1/7.5 g/mL), stirring speed of 320 rpm at leaching temperature of 50 ℃ in 60 minutes.

The sulphuric acid roasting method offers a promising way of extracting lithium as lithium carbonate from the Zimbabwean petalite. The experimental results show that purity of Li_2CO_3 produced by this process was 99.21 % (metal basis). XRD of the synthesised powder indicate that no other phases were present except of zabuyelite (Li_2CO_3). The thermograms for synthesised and commercial Li_2CO_3 where almost identical with both powder starts decomposing around 725 ℃. The average particle size of the synthesised Li_2CO_3 is 1.4 µm with the corresponding surface area of 5.3 m^2/g.

Good quality LiF with cubic morphology can be produced by precipitation with a LiF content of > 99 %. This was well supported by XRD results which show that no other phase was present except of griceite (LiF). The major impurity is Na. The pH, concentration and agitation have a great influence on the morphology of the precipitated LiF. Lower pH values, optimum concentration of Li_2CO_3 solution results in smaller particle size. Agitation of the solution results in less agglomerated particles.

Higher temperature values of around 80 °C are not suitable for preparation of LiF as Li_2CO_3 in solution re-precipitates affecting the quality of the product. High recovery of 96.53% LiF was realised using this process.

Anhydrous LiCl of 99.02 % purity was produced. LiCl was found to absorb moisture when exposed to air at ambient temperature. Melting of the synthesised LiCl occurs at 606.2 °C and the corresponding enthalpy of fusion was 18.4 kJ mol^{-1}. Evaporation for both synthesised and Merck LiCl took place at temperatures below the nominal boiling point of LiCl.

Zimbabwean petalite indeed represents a strategically-important potential source of lithium and lithium compounds, as a result of the increase in demand for lithium and lithium compounds necessitated by an increase in demand for lithium-ion batteries. There is no doubt that lithium recovery from sources such as Bikita petalite explored in this research would be of importance.

5.2 Recommendations

The following recommendations are suggested for further investigations which could help in processing of Zimbabwean petalite to obtain high purity lithium salts.

- Further processing of lithium carbonate is necessary in order to produce high purity lithium salts of purity > 99.99 %, suitable for pharmaceutical applications, production of electronic grade crystals or preparation of battery-grade lithium metal and lithium hexafluorophosphate. Methods for purifying lithium carbonate have been reported in literature such as removal of impurities in Li_2CO_3 by ion-exchange (Amouzegar, 2000) or liquid-liquid extraction (Yi et ., 2007).
- Recovery of sodium sulphate as a marketable product from the lithium carbonate mother liquor should be investigated further.
- Economic viability of the lithium carbonate production process needs to be evaluated.

REFERENCES

- Alvani, C, Casadio, S, Contini, V, Bartolomeo, A.D, Lulewicz, J.D and Roux, N (2002) " Li_2TiO_3 peddles reprocessing, recovery of ^6Li as Li_2CO_3" *Journal of Nuclear of Materials*, 307(1), 837-841.

- Amouzegar, K, Amant, G.S and Harrison, S (2000) "Process for the purification of lithium carbonate" *U.S Patent*, 6 048 507, assigned to Limtech, Cape Rouge, Canada.

- Amer, A.M (2008) "The hydrometallurgical extraction of lithium from Egyptian Montmorillonite-type clay" *Journal of Minerals*, 60(10), 55-57.

- Anderson, E.R (2009) "Lithium supply and market conference, Chile 2009). Available at <http:trugroup.com/Lithium-Market-Conference. html> (accessed on 15.05.2010).

- Anovitz, L.M, Blencoe, J.G and Palmer, D.A (2006) "Method of extracting lithium" *U.S Patent,* 0 171 869 A1, assigned to Macmillan, Sobanksi and Todd, US.

- Averill, A.W and Olson, D.L (1977) "A review of extractive process for lithium from ores and brines" *Energy*, 3(3), 305-313.

- Azaroff, L.V (1968) *Elements of X-ray Crystallography*, McCraw-Hill Book Company, New York.

- Bale, M.D and May, A.V (1989) "Processing of ores to produce tantalum and lithium" *Minerals Engineering* 2(3), 299-320.

- Bannett, H and Oliver, G (1992) *XRF Analysis of Ceramics, Minerals and Applied Material,* John Wiley and Son, New York, United States of America.

- Boss, C.B and Fredeen, K.J (1999) *Concepts, Instrumentation and Techniques in Inductively Coupled Plasma Optical Emission Spectrometry*, 2nd edition, Perkin-Elmer Corp., USA.

- Boumans, P.W.J.M (1987) *Inductively Coupled Plasma Optical Emission Spectrometry- Methodology Instrumentation and Performance*, John Wiley and Sons, New York.

- Brandt, F and Haus, R (2010) "New concepts for lithium minerals processing" *Minerals Engineering*, 23(8), 659-661.

- Brown, M.E (2001) *Introduction to Thermal Analysis*, Kluwer Academic Publisher, London.

- Brown, M.E (1988) *Introduction to Thermal Analysis*, Chapman and Hall, London.

- Burkert, G.M and Ellestad, R.B (1970) "Precipitation of lithium carbonate from lithium chloride solution" *US Patent* 3523751, assigned to Lithium Corporation of America.

- Buyukburc, A, Maraslioglu, D, Bilici, M.S and Koksal, G (2006) "Extraction of lithium boron clays by using natural and waste materials and statistical modelling to achieve cost reduction" *Minerals Engineering*, 19(5), 515-517.

- Charsely, E.L and Warrington, S.B (1992) *Thermal Analysis*, The Royal Society of Chemistry, Cambridge.

- Chemetall (2009) “Chemetall statement: Application and availability of lithium”. Available at <www.chemetalllithium.com> (accessed on 21.11.2010).

- Comer, E.P (1978) “The lithium industry today” *Energy*, 3(3), 237-240.

- Conde, M.R (2004) “Properties of aqueous solutions of lithium and calcium chlorides: formulations for use in air conditioning equipment design” *International Journal of Thermal Sciences*, 43*(1)*, 367-382.

- Connolly, J.R (2007) *Introduction to X-ray Powder Diffraction*, Spring.

- Cooper, D.G (1964) S*ome ore deposits in Southern Africa, the geology of the Bikita pegmatite*, Geology Society of South Africa, Vol. II.

- Coulson, J.M and Richardson, J.F (1996) *Chemical Engineering-Particle Technology and Separation Process*, Butterworth-Heinemann, Oxford.

- David, R. L (2009) *Handbook of Chemistry and Physics, 89th Edition,* CRC Press/Taylor and Francis, Boca Raton, FL.

- Distin, P.A and Philips, C.V (1982) “The acid extraction of lithium from the granites of South West England” *Hydrometallurgy*, 9(1), 1-14.

- Demirbas, A (1999) “Recycling of lithium from borogypsum by leaching with water and leaching kinetics” *Resources, Conservation and Recycling*, 25(2), 125-131.

- Ebensperger, A, Maxwell, P and Moscoso, C (2005) “The lithium industry: Its recent evolution and future prospects” *Resource Policy*, 30(3), 218-231.

- Eccelestone, C (2010) “Lithium sector review: Life in the lithosphere” Hallargeten and Company. Available at <www.hallagartenco.com> (accessed 24.11.2010).

- Epstein, J.A, Feist, E.M, Zmora, J and Marcus, Y (1981) “Extraction of lithium from the Dead Sea” *Hydrometallurgy*, 6(3-4), 269-275.

- Friedrich, H, Pfeffinger, J and Leutner, B (1999) “Method for producing highly pure lithium salts” *US Patent* 6 592 832, assigned to BASF Aktiengesellschaft, Ludwigshafen.

- Garrett, D.E (2004) *Handbook of Lithium and Natural Calcium Chloride*, Elsevier, Oxford.

- Grady, H.R (1980) “Lithium metal for the battery industry” *Journal of Power Sources*, 5(1), 127-135.

- Jackson, E (1986) *Hydrometallurgical Extraction and Reclamation*, Ellis Horwood Ltd, Chichester.

- Jandová, J, Dvorák, P, Vu, H.N (2010) “Processing of zinnwaldite waste to obtain Li_2CO_3” *Hydrometallurgy*, 103(1), 12-18.

- Jandová, J, Vu,H.N, Belková, T, Dvorák, P (2008) “Lithium extraction from zinnwaldite wastes using the gypsum method” *Acta Metallurgica Slovaca*, 14(1), 101-105.

- Jaskula, B.W (2010) U.S. Geological Survey, Mineral commodity summaries lithium: U.S. Geological Survey 2010, 92-93. Available at<http://minerals.usgs /gov/minerals/pubs/mcs/2010/mcs 2010.pdf> (accessed on 2.7.2010).

- Jaskula, B.W (2008) Lithium, Minerals Yearbook-2007, U.S. Geological Survey, 2008, 44.1-44.8. Available at <http://minerals.usgs .gov/minerals/pubs/commodity/lithium/myb1-2007-lith.pdf>(accessed on 2.7.2010).

- Habashi, F (1997) *A Handbook of extractive Metallurgy*, Volume (IV), WILEY-VCH, New York.

- Hamazaoui, A.H, M'nif, A, Hammi, H and Rokbani, R (2003) "Contribution to the lithium recovery from brine" *Desalination*, 158 (1-3), 221-224.

- Kamali, R.A, Fray, D.J and Schwandt, C (2011) "Thermokinetic characteristics of lithium chloride" *Journal of Thermal Analytical Calorimetry*, 104(2), 619-626.

- Kamiensiki, C.W, McDonald, D.P, Stark, M.W and Papcun, J.R (2005) "Lithium and lithium compounds", in *Kirk-Othmer, Encyclopedia of Chemical Technology*, vol. 15, John Wiley and Sons, New Jersey.

- Karell, E.J, Grourishankar, K.V, Smith, J.L, Chow, L.S and Redey, L (2001). "Separation of actinides from LWR spent fuel using molten-salt-based electrochemical processes" *Nuclear Technology*, 136(3), 342-352.

- Kitazawa, S, Choi, Y, Yamamoto, S and Yamaki, T (2006) "Rutile and anatase mixed crystal TiO_2 thin films prepared by pulsed laser deposition" *Thin Solids Films*, 515(4), 1901-1904.

- Kondás, J and Jandová, J (2006) "Lithium extraction from zinnwldite waste after gravity dressing of Sn-W ores" *Acta Metallurgica Slovaca*, 12(1), 197-202.

- Lagos, S and Becerra, R (2005) “Methodology for the recovery of lithium from lithium titanate” *Journal of Nuclear Materials*, 347(1-2), 134-139.

- Levenspiel, O (1972) *Chemical Reaction Engineering*, Wiley, New York, NY.

- Loubser, M and Verryn, S (2008) “Combining XRF and XRD analyses and sample preparation to solve mineralogical problems” *South African Journal of Geology*, 56(III), 229-238.

- Mcketta, J.J (1988) “Lithium and lithium compounds”, in *Encyclopedia of Chemical Processing and Design*, Vol.28, Marcel Dekker.

- Mobbs, P.M (1995) The Mineral industry of Zimbabwe, U.S. Geological Survey. Available at <http://minerals.usgs.gov/minerals/pub/ country/maps/-92469.gif> (accessed on 2.9.2010).

- Montaser, A and Golightly, D.W (1992) *Inductively Coupled Plasmas in Analytical Atomic Spectrometry*, 2nd edition, CHC, New York.

- Nicholson, P (1978) “Past and future development of the market for the lithium in the world aluminium industry” *Energy*, 3(3), 243-246.

- Ober, J.A (2007) “Lithium, Minerals Yearbook-2006, U.S. Geological Survey, 2007, 44.1-44.7. Available at <http://minerals.usgs.gov/ minerals/pubs/commodity/lithium/lithmyb06.pdf> (accessed on 2.7.2010).

- Postek, M.T, Howard, K.S, Johnson, A.H and McMichael, L.L (1980) *Scanning Electron Microscopy: A Student Handbook*, Ladd Research Industries, Williston, VT.

- Roering, C and Gevers, T.W (1964) *Some ore deposits in Southern Africa, Lithium and Beryllium-bearing pegmatite in Karibib district, South West Africa*, Geology Society of South Africa, Vol. II.

- Sarraf-Mamoory, R, Nadery, S and Riahi-Noori, N (2007) "The effect of precipitation of lithium fluoride (LiF) nano-powder" *Chemical Engineering communications,* 198(8), 1022-1028.

- Selby, M, Sturman, B and Willis, J.B (1991) *Analytical Methods for the Liberty Spectrometer*, Varian Australia Pty. Ltd.

- Smith, K (1990) *Soil Analysis Modern Instrumental Techniques*, 2nd edition, Marcel Dekker Incl, New York.

- Stoch, H (1986) *A manual of Analytical Methods used at Mintek,* Randburg, Council for Mineral Technology.

- Thompson, M and Walsh, J.D (1989) *Handbook of Inductively Coupled Plasma Spectrometry*, 2nd edition, Blackie and Son.

- Thorpe, T.E (1922) *A Dictionary of Applied Chemistry*, Volume 4, Longman, Green and Co. London.

- Varnes, A (1997) *Inductively Coupled Plasma Atomic Emission Spectroscopy, Hand book of Instrumental Analysis for Analytical Chemistry*, Ed. Settle, Frank, New Jersey: Prentice Hall, 1997.

- Veasey, T.J (1997) "A review of the minerals industry in Zimbabwe" *Minerals Engineering* 10(12), 1355-1362.

- Wandlandt, W.W (1986) *Thermal Analysis*, Wiley, New York.

- Wang, R-C, Lin, Y-C and Wu, S-H (2009) “A novel recovery process of metal values from the cathode active materials of the lithium-ion secondary batteries” *Hydrometallurgy*, 99(3-4), 194-201.

- Watson, J.P (1996) “Fast, simple method of powder pellet preparation for X-ray fluorescence analysis” *X-ray Spectrometry*, 25(4), 173-174.

- Wietelmann, U and Bauer, R.J (2003) “Lithium and lithium compounds”, in *Ullmann’s Encyclopedia of Industrial Chemistry*, Vol.20, WILEY-VCH Verlag GmbH & Co. Weinheim, Germany.

- Yi, W.T, Yan, C.Y, Ma, P.H, Li, F.Q and W, X.M (2007) “Refining of crude Li_2CO_3 via slurry phase dissolution using CO_2” *Separation and Purification Technology*, 56(3), 241-248.

- Zhang, P, Yokoyama, T, Itabashi, O, Suzuki, T.M and Inoue, K (1998) “Hydrometallurgical process for the recovery of metal values from spent lithium-ion secondary batteries” *Hydrometallurgy,* 47(2-3), 259-271.

APPENDICES

APPENDIX A: Analytical techniques

The following analytical techniques were used in this study.

A.1 X-ray diffraction (XRD)

X-ray diffraction analysis (XRD) is the common tool for investigating the structure of crystalline materials, from atomic arrangement to crystallite size by observing the pattern in which they scatter a beam of rays. During X-ray diffraction analysis, the X-ray beams are reflected off the parallel atomic layers within a sample over a range of diffraction angles. Because the X-ray beam has a specific wavelength, for any given “d-spacing” (distance between adjacent planes) there are specific angles at which the exiting rays will be in phase and therefore, will be picked up by the detector producing a peak on the diffractogram (Azaroff, 1968). Just like a fingerprint, every mineral compound has its own set of diffraction peaks to identify it. The X-ray detector moves around the sample and measures the intensity of these peaks and the position of these peaks (diffraction angle 2θ). The highest peak is defined as the 100% peak and the intensity of all the other peaks are measured as a percentage of the 100% peak. Schematic diagram of a diffractometer system is shown on Figure 32 (Connolly, 2007).

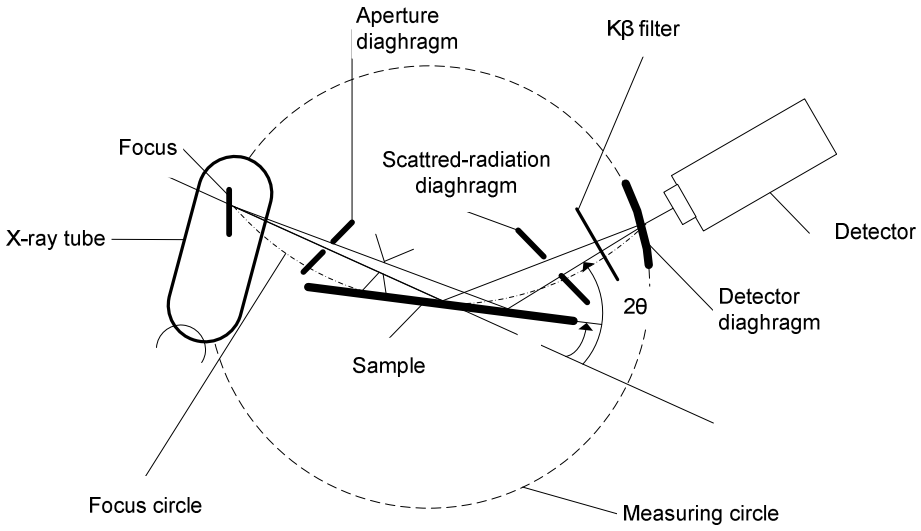

Figure 32. A schematic diagram of an X-ray diffractometer.

The diffracted beams from atoms in successive planes cancel unless they are in phase, and the condition for this is given by the Bragg relationship as in equation 15 (Connolly, 2007). The rays of the incident beam are always in phase and parallel up to the point at which the top beam strikes the top layer at atom z as shown on Figure 33. The second beam continues to the next layer where it is scattered by atom B. The second beam the extra travel the extra distance AB + BC. This extra distance must be an integral (n) multiple of the wavelength (λ) for the phases of the two beams to be the same.

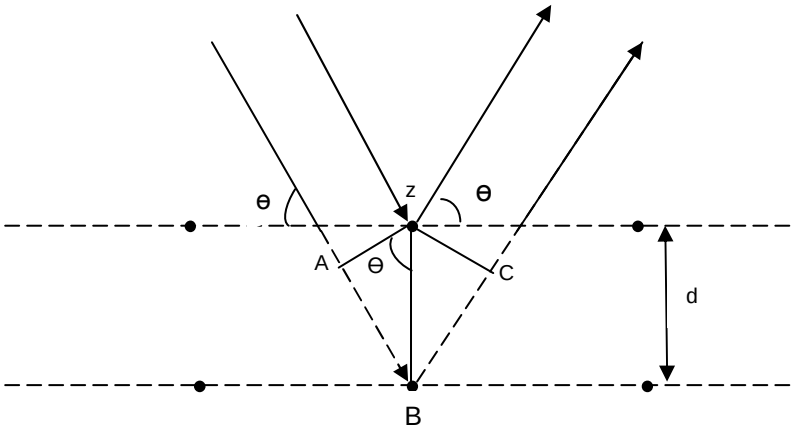

Figure 33. Scattered beam of X-rays.

The Bragg condition is

$$n\lambda = 2d\sin\theta \tag{17}$$

λ is the wavelength of the equation d is the distance between difference plane of atoms in a crystal structure, θ is the angle of diffraction, n is the order number.

Crystalline size can also be estimated from XRD patterns using the Scherrer equation (18) (Kitazawa et al., 2008). This does not however consider the effect that micro-stresses have on the peak width.

$$t = \frac{\kappa\lambda}{\beta\cos\theta} \tag{18}$$

κ is a constant which is frequently taken as 0.9, t is the particle dimension
β is the peak width in radians and λ is the wavelength of X-ray.

A.2 X-ray fluorescence (XRF)

X-ray fluorescence spectroscopy is used to determine chemical composition of a sample. Elements from fluorine to uranium in the periodic table can be analysed using XRF. XRF has the advantage of being non-destructive, multi-elemental, fast and cost effective. However the major drawback is that analyses are restricted to elements F to U (Bannett and Oliver, 1992). The XRF principle is shown in Figure 34.

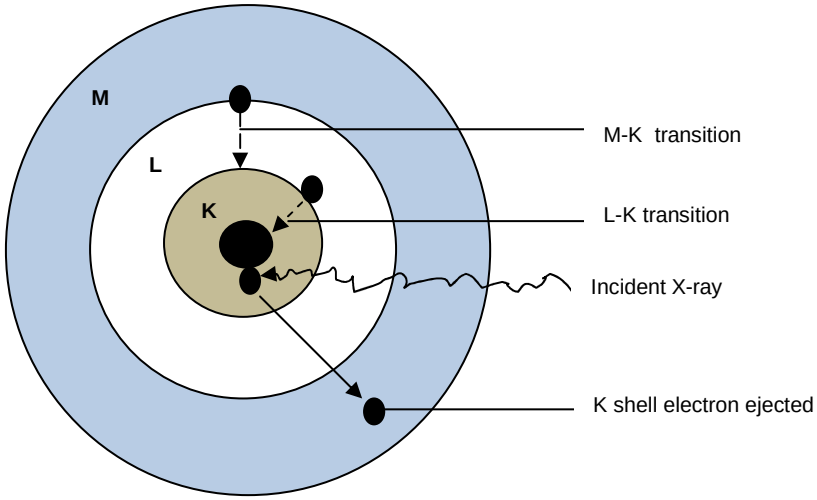

Figure 34. X-ray fluorescence principle.

An inner shell electron is excited by an incident photon in the X-ray region. During the de-excitation process, an electron moves from a higher energy level to fill the vacancy. The energy difference between the two shell appear as an X-ray emitted by an atom. The X-ray spectrum acquired during the above process reveals a number of characteristics peaks. The energy of the peaks leads to the identification of the elements present in the sample (qualitative analysis) and the peak intensity provides the relevant or absolute elemental concentration (semi-quantitative or qualitative analysis).

Sample preparation involves milling the sample in a tungsten carbide milling pot to a particle size below 75 μm. The samples are dried at 110 °C (weight 1) and roasted at

1000 °C (weight 2), to determine the percentage loss on ignition (LOI) using the following equation (19) (Laubser and Verryn, 2008):

$$\%LOI = \frac{weight_1 - weight_2}{weight_1 - crucibleweight} x100 \quad (19)$$

Analysis of trace elements is done on pressed powder pellets. A finely ground sample is mixed with a small amount of saturated solution of polyvinyl alcohol (binder) to enhance sample strength. To facilitate handling, the sample is pressed in a thin aluminium container to form pellets at pressure of 20 ton cm^{-2}. The sample is then dried at 110 °C before analyses are done.

Major element analyses are done on fused beads. This method has the advantage that fusion destroys the mineral grains and their structures thus distributing constituents elements homogenously throughout the mass eliminating the grain size effect, and dilution reduces errors introduced by mass absorption. If there is undissolved material, it is all retained in the bead which can be re-melted (Watson, 1996). Pre-roasted sample is added to lithium tetraborate ($Li_2B_4O_7$) flux mixed in a 95 % Pt, 5 % Au crucible and fused at 1000 °C in a muffle furnace automated fluxer. A mouldable crucible is used so that, on removal from the furnace the bead is fast cooled in the crucible of which the bottom surface is analysed (Watson, 1996).

A.3 Scanning electron microscope (SEM)

The scanning electron microscope gives high resolution images of the morphology and topography of a specimen. SEM also gives the chemical composition and crystallographic information.

The microscope uses a monochromatic electron beam that travels downward through a series of magnetic lenses designed to focus the electrons to a very fine spot. An electron gun which is mainly located at the top of the machine is used to fire a beam of electrons. The most common type of gun used are the thermionic type which applies thermal energy to a filament to coax electrons away from the gun towards the specimen. The filament controls the number of electrons leaving the

gun. The beam of electrons is scanned across the sample and secondary electrons are emitted from its surface. Secondary electrons from the specimen are attracted to the detector by positive charge (Postek et al., 1980). A detector counts these electrons and sends the signals to an amplifier. The final image is built up from the number of electrons emitted from each spot on the sample. A schematic diagram of a scanning electron microscope is shown on Figure 35 (Postek et al., 1980).

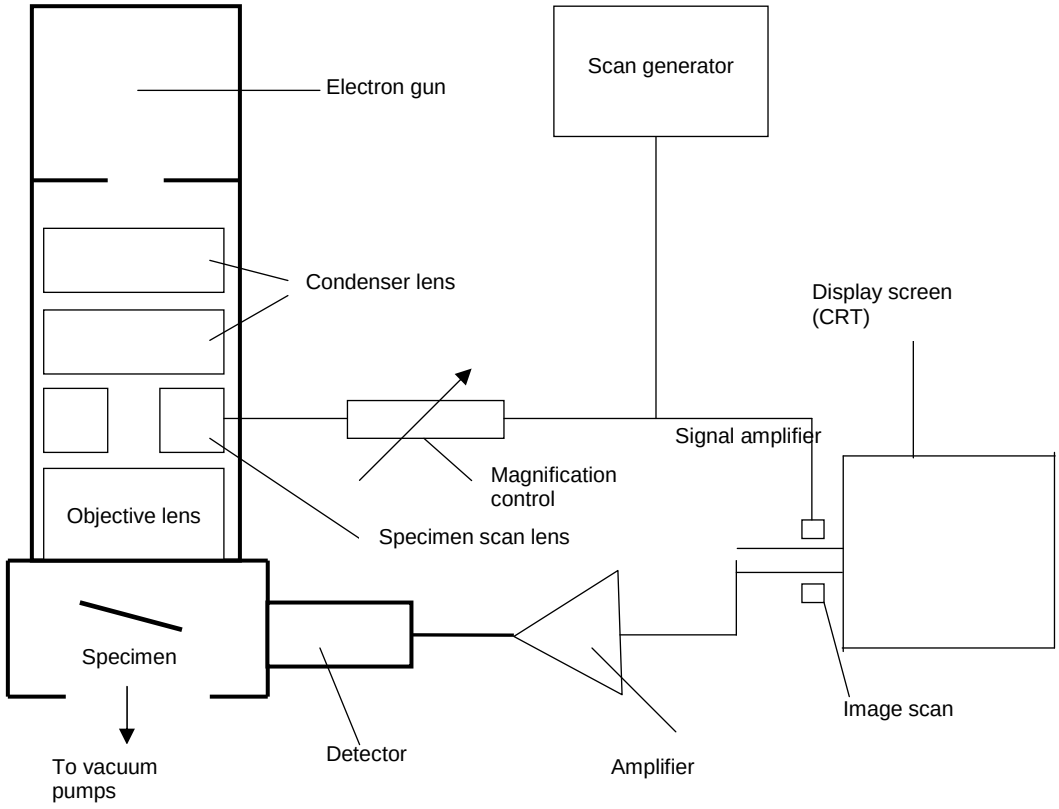

Figure 35. Schematic diagram of a scanning electron microscope.

A.4 Inductively coupled plasma optical emission spectrometry (ICP-OES)

An ARCOS model, Inductively Coupled Plasma Optical Emission Spectrometer (ICP-OES), from SPECTRO was used for the determination of lithium and other elements in solution. ICP-OES uses high energy argon plasma to convert elements in a

sample solution into gaseous, excited form that emits electromagnetic radiation at characteristic wavelength. The colours of the emitted light and the light intensity are used to identify the element and quantify its concentration. The ICP-OES uses an array detector so that many elements in a sample can be determined simultaneously. The fundamental characteristic of this process is that each element emits energy at multiple wavelengths and in the ICP-OES technique it is ideal to select the recommended lines for a given element. Commonly used lines for an element depend on the sensitivity of the line and if there is possible interferences (Thompson and Walsh, 1989). ICP-OES has the advantages of: high sample throughput; multiple element measurements in the same run; detection of low concentrations; accuracy; and less susceptible to interferences than comparable spectrometric techniques.

A typical ICP-OES system consists of the following components:

- Sample introduction system
- The plasma, ICP torch and the gas supply
- Radiofrequency generator
- Transfer optics and optical spectrometer
- Detector
- Computer

Figure 36 shows a schematic diagram of an inductively coupled plasma optical emission spectrometer.

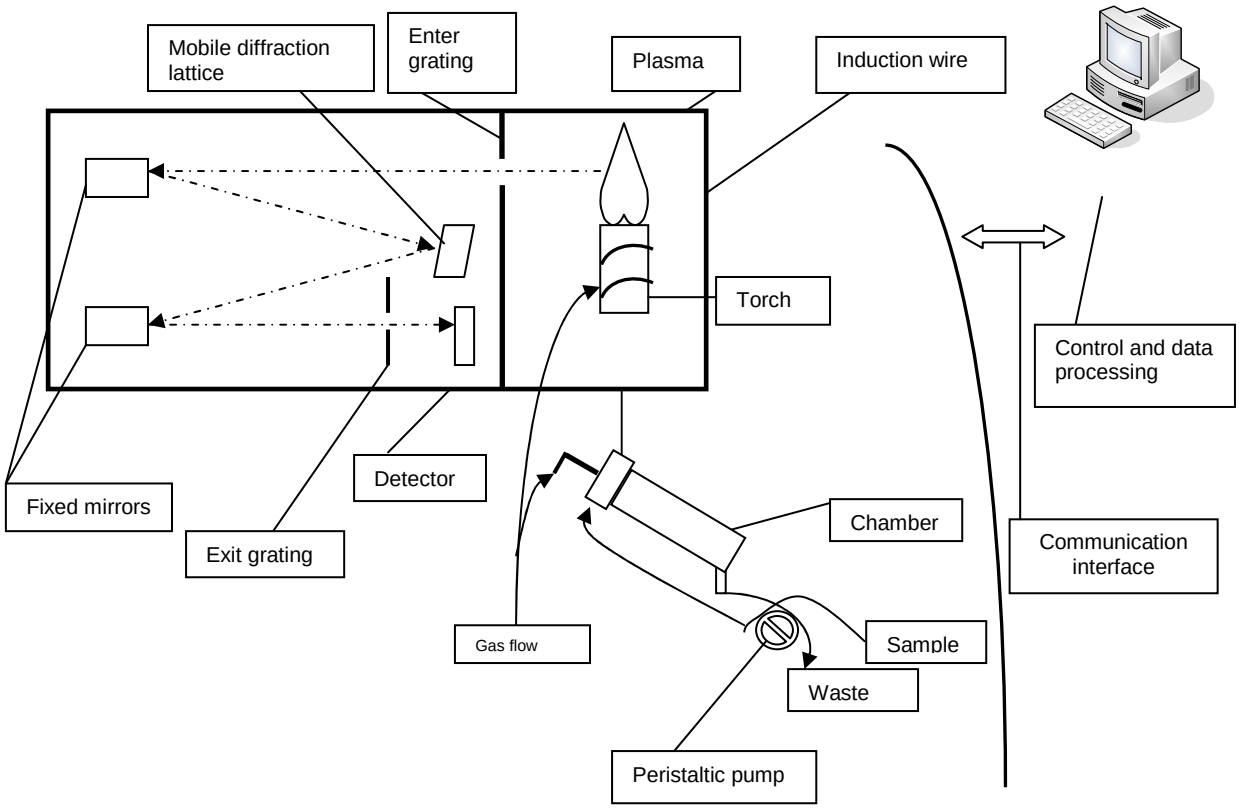

Figure 36. Schematic representation of an ICP-OES instrument.

Sample introduction system

The sample introduction system consists of the peristaltic pump for the sample uptake, nebulizer to aspirate the sample and the spray chamber to separate the smaller from bigger droplets. The smaller droplets (1-10 µm) are transferred by argon gas flow into the heart of the ICP-OES, the argon plasma. The bigger droplets (>90 %) are pumped out as waste. There are different instrument designs and the selection of the ideal one is dependent upon the type of sample to be analysed and the sensitivity required.

Peristaltic pump: The peristaltic pump is used for the transport of the sample from the sample container to the nebulizer's sample inlet connection. The peristaltic pump uses the compression and release of pump tubing to transport the sample (Boss and Fredeen, 1999). The diameter of the tubing and rotational speed of the pump can be

selected to transport a large or small volume of sample. The pump must have a consistence feed rate, this means that surges in feed rate must be avoided. The peristaltic pump has the ability to rinse the system and wash the sample quicker. This aspect saves on the analysis time without compromising stability of the instrument. Figure 37 shows a typical image of a peristaltic pump for a Spectro Arcos ICP-OES.

Figure 37. Peristaltic pump.

Nebulizer: The fluid sample is pumped into the nebulizer via peristaltic pump. The nebulizer generates a primary aerosol mist in argon with typical droplet size in the range of below ten to hundred micrometers (Thompson and Walsh, 1989). The mist accumulates in the spray chamber, where the largest mist particles settle out as waste and the finest particles subsequently swept into the torch assembly.

There are two types of main categories of nebulizers: pneumatic and non-pneumatic or ultrasonic (Thompson and Walsh, 1989). Pneumatic nebulizers are the most frequently used and are recommended only for clean samples, since the inner capillary can be clogged by particles or high concentrations of salts. This type of nebulizer offers excellent sensitivity and stability. An example of pneumatic nebulizer is concentric nebulizer. A concentric nebulizer is shown on Figure 38.

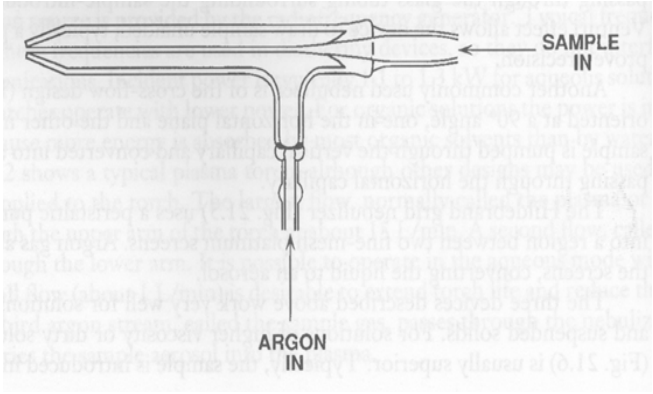

Figure 38. Concentric nebulizer (Adapted from Varnes, 1997).

The cross flow nebulizer is another type of a pneumatic that is used for general purpose or multipurpose since the parts are made from inert materials. It can handle materials such as hydrofluoric acid and organic materials. Ultrasonic nebulizer, this type of neubilizer has high detection limit compare to pneumatic nebulizers. Typical detection limits can be improved by a factor of 5 to 25, depending on the analyte (Montaser and Golightly, 1992).

Spray chamber: The spray chamber's main function in the sample introduction system is to remove the large droplets from the nebulizer. This is achieved through gravitational and centrifugal forces allowing only droplets of suitable size (about 10µm) to continue on their path to the plasma. The large droplets are condensed in the spray chamber and led to the waste container. A small positive pressure is necessary to drive the aerosol into the injector tube. The mostly widely used spray chamber is the double
pass Scott type (Thompson and Walsh, 1989). Figure 39 shows an image of a double pass spray chamber for a Spectro Arcos with the ability to handle HF.

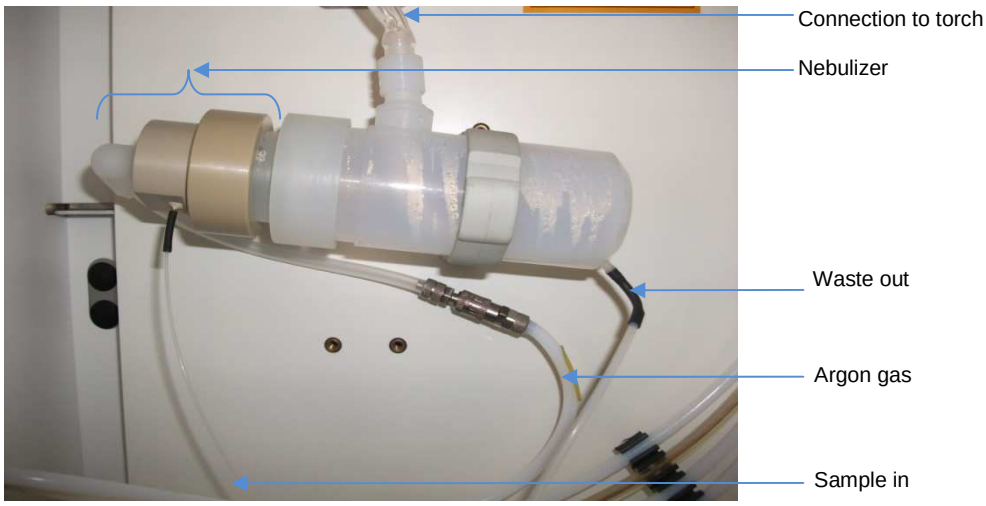

Figure 39. Spray chamber connected to the neubilizer.

The plasma, ICP torch and the gas supply

The inductively coupled plasma (ICP): An ICP is formed during the coupling of free electrons from an argon gas to the energy radio frequency (RF) magnetic field, which is produced by the radio frequency generator (1-3 kW power at 27-50 MHz). The gas is contained in a plasma torch, which is constructed from materials that are resistance to high temperature and is transparent to the RF radiation. The most commonly used material for this purpose is quartz. The magnetic field is generated by a silver plated copper coil that is placed around the upper part of the torch. The initial electrons needed to ignite the plasma are provided by an internal spark discharge. In the plasma, the electrons are accelerated by the field magnetic field oscillation. This in turn results in effective energy transfer from the field to the electrons. When equilibrium is reached between the rate of electrons production and the loss resulting from recombination and diffusion, the plasma is stable and can be used for analytical measurements (Smith, 1990).

The plasma has different zones of importance, viz. the preheating zone, the initial radiation zone, induction and the hotter normal analytical zone (6000-10000K) as indicated on Figure 40 (Selby et al.,1991). These zones are not fixed in position and are influenced by the operating conditions. Several parameters play an important

role in the position of the different zones in the plasma which are the applied power and sample carrier gas flow, quantity and particle size distribution of the aerosol and the matrix component of the sample.

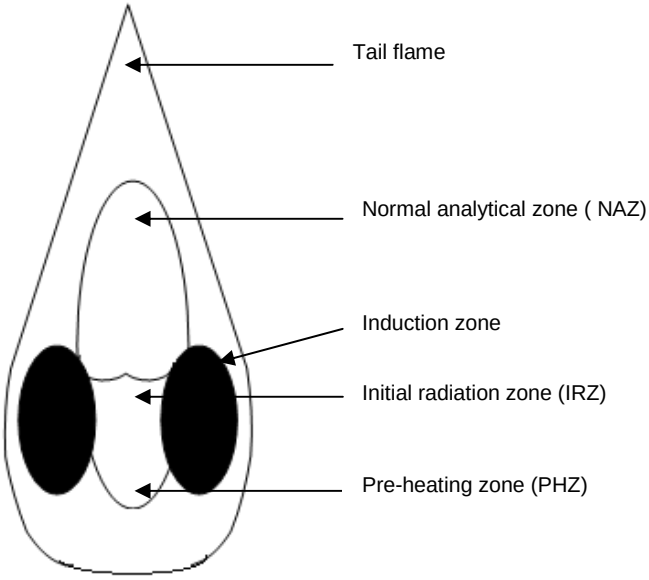

Figure 40. Schematic representation of the different zones in the ICP.

The ICP torch: The ICP torch sustains the plasma of the ICP-EOS. The torch consists of three concentric quartz tubes arranged to provide suitable gas flow geometry. ICP torches are of two types which are: Scott-Fassel and demountable type (Smith, 1990). The Scott-Fassel type is the most common one and was used in the experimental setup of this study. This type of torch requires high degree of concentricity. The main disadvantage of this type of tube is that when the injector tube or outer tube in the vicinity of the plasma is damaged, the whole torch has to be replaced and to replace a torch is costly. The demountable torch consists of the inner, outer and injector tube. In contrast to the Scott-Fassel type this torch can be fully disassembled and the damaged parts can be replaced individually. The inner and outer tubes are housed in a body made up of a ceramic-loaded Teflon (PTFE) for thermal stability (Smith, 1990). The sample introduction tube and the injector

mounting are made of normal PTFE. The orientation of the torch can be radial or axial. Figure 41 shows an image of a touch for a Spectro Arcos.

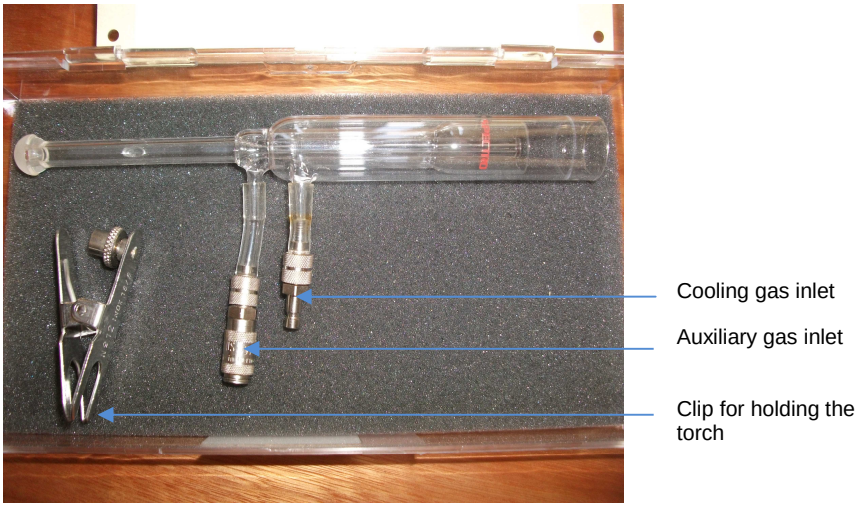

Figure 41. An image of a torch for Spectro Arcos.

Radio frequency generator

The radio frequency generator produces energy radio frequency (RF) magnetic field at frequencies 27-50Mz which couples with free electrons from argon gas to form plasma. The RF generator provides power (1-3 kW) through induction coil (copper coil) which surrounds the top end of the touch to the plasma. During operation the coil is cooled by the gas or water (Selby et al., 1991). When RF power is applied to the coil, alternating current oscillates at a rate corresponding to the frequency of the generator (Boumans, 1987).

Transfer optics

Monochromator, its purpose is to isolate emitted lines. It can either be prisms or gratings. Grating monochromator uses diffraction along grated surface to reinforce the light**.**

Detectors

A photosensitive detector such as photomultiplier tube (PMT) or a charge-injection device (CID) detector is used. Detectors are aligned to receive the spectral emission. In grating monochromators, they are along focal points.

A.5 Thermogravimetric analysis (TGA)

The instrument used in thermogravimetric analysis (TGA) is called a thermobalance. In this technique, change in mass (mass loss or gain) is determined as a function of temperature (Wendlandt, 1986). Figure 42 shows a schematic diagram of a thermobalance (Brown, 1988).

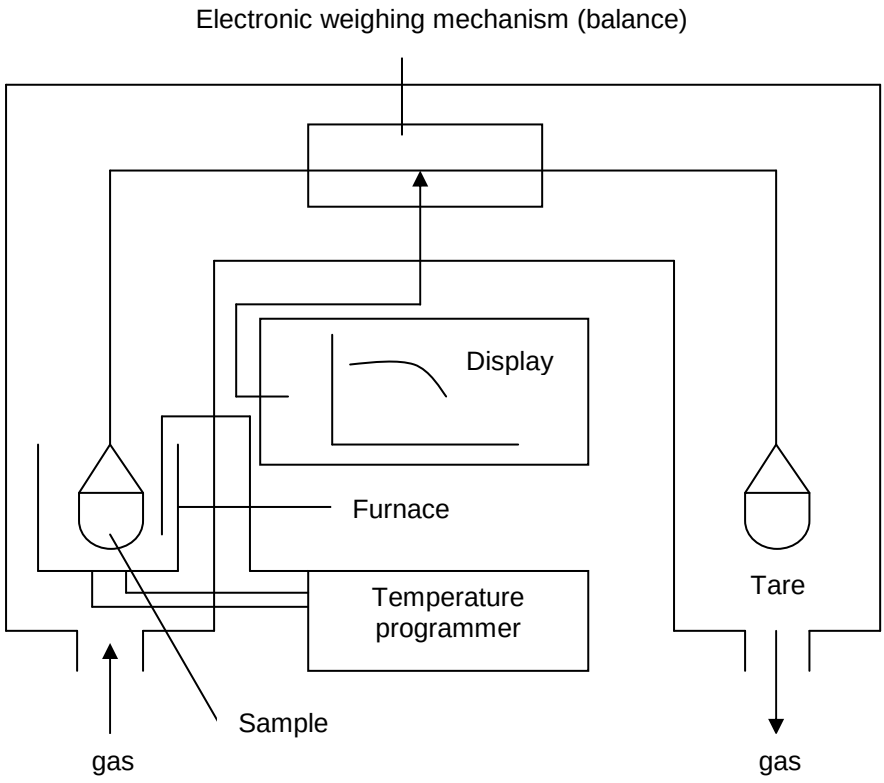

Figure 42. A schematic diagram for a thermobalance.

The thermobalance consists of four basic components in order to provide the flexibility necessary for the production of useful analytical data in the form of TGA curve.

These basic components are as follows:

i) Balance

ii) Furnace

iii) Unit for temperature measurement and control (programmer)

iv) Recorder

- **Balance**

The balance should have the following characteristics: accuracy, sensitivity, reproducibility, and capacity. A number of balance mechanisms are available which includes beam, spring, cantilever and torsion (Brown, 1988). These balance mechanisms can grouped into two types, viz. null point and deflection type (Charsely and Warrington, 1992). The null-point weighing mechanisms is favoured in TGA as they ensure that the sample remains in the same zone of the furnace irrespective of changes in mass (Brown, 2001).The null type balance incorporates a sensing element which detects a deviation of the balance beam from its null position. A sensor detects the deviation and triggers the restoring force to bring the balance beam to back to the null position. The restoring force is directly proportional to the mass change. Deflection balance of the beam type involves the conversion of the balance beam deflection about the fulcrum into a suitable mass-change trace. The different balances used in TG instruments have measuring ranges of 1 μg to 1 g (Brown, 1998).

- **Furnace**

The furnace and control system is designed to produce linear heating over the whole working temperature range. A temperature range generally -150 ℃ to 2000 ℃ of furnaces is used in different instruments depending on the model. The desirable features of a furnace include: having a uniform hot-zone of reasonable length, reaching the required temperature as quickly as possible, not affecting the balance mechanism through radiation or convection, a recorded temperature identical to the sample temperature (Charsely and Warrington, 1992; Brown, 1998)

- **Temperature measurement and control**

Temperature measurements are commonly done using thermocouples (Charsely and Warrington, 1992). Chromal-alumel thermocouple is often used for temperature up to 1100 ℃ whereas Pt or (Pt-10 % Rh) is employe d for higher temperatures.

Temperature is controlled or varied using a program controller with two thermocouple arrangement. The signal from one thermocouple controls the system whilst the second thermocouple records the temperature.

- **Recorder**

The automatic recording unit logs for the mass and temperature changes. Graphic recorders are preferred to meter type recorders. X-Y recorders are commonly used as they plot weight directly against temperature (Brown, 2001; Charsely and Warrington, 1992). The balance output and thermocouple signal are fed to the recorder to generate the TG curve.

APPENDIX B: Integrated heat flow peaks

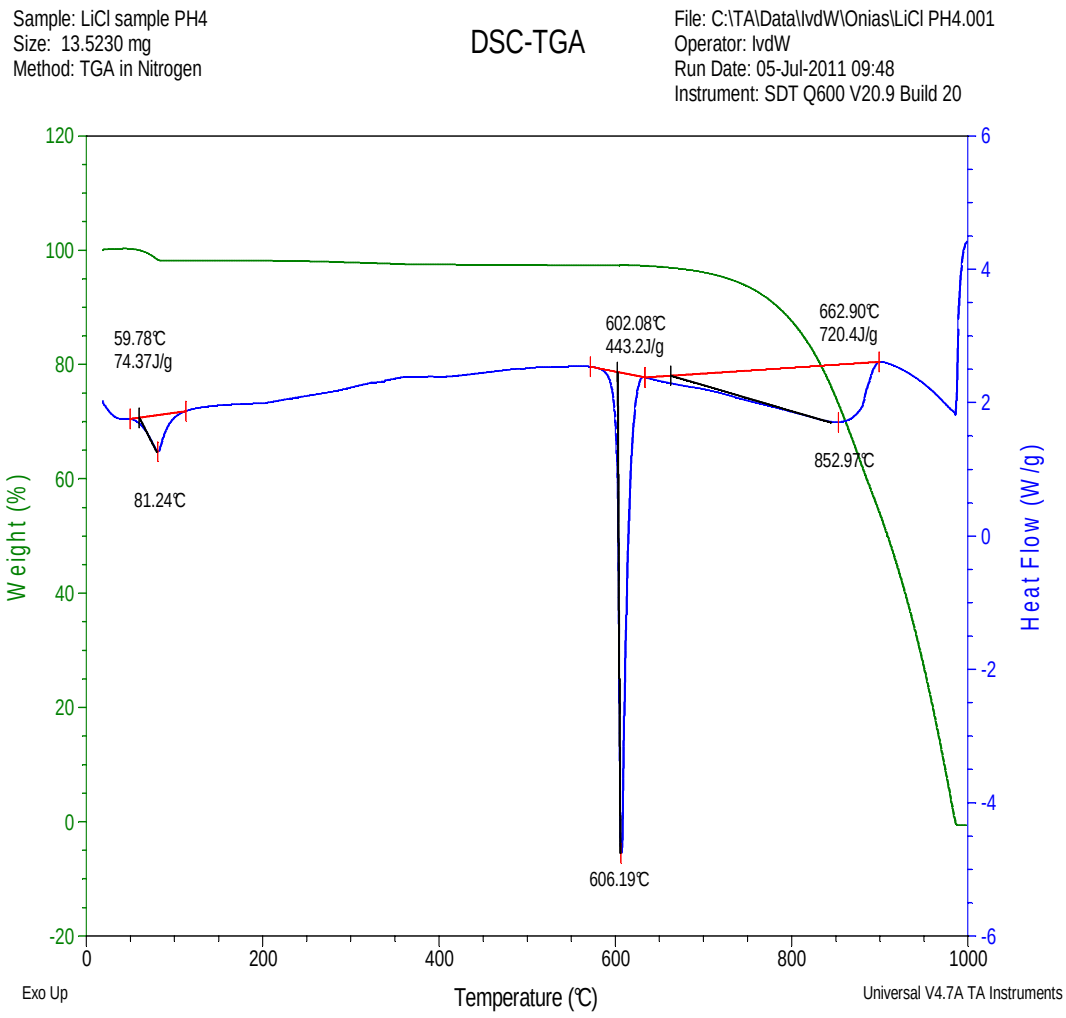

Figure 43. Integrated heat flow peaks for synthesised LiCl.

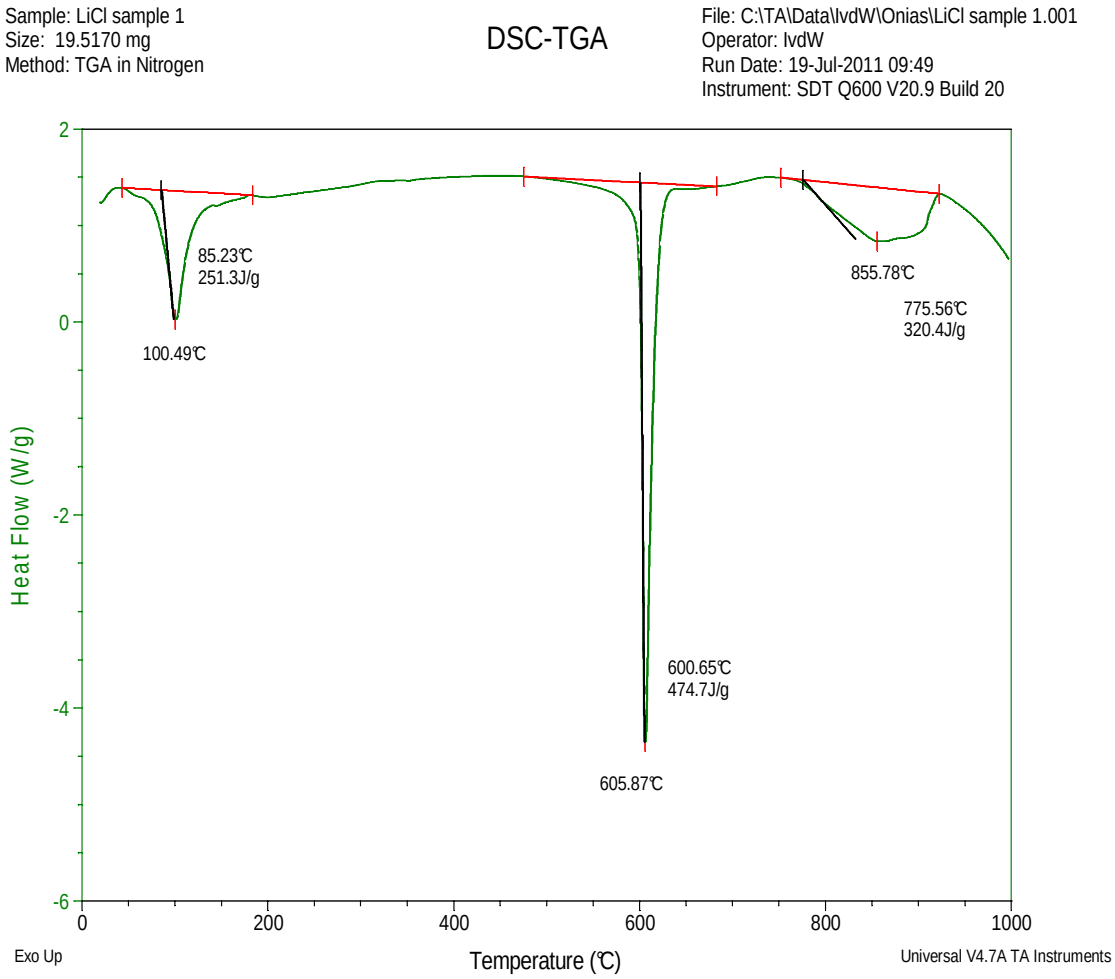

Figure 44. Integrated heat flow peaks for purchased LiCl.